Faculteit Industriële Ingenieurswetenschappen

master in de industriële wetenschappen: chemie

Masterthesis

Evaluating the impact of reprocessed content and multiple reprocessing cycles on the performance of polyethylene stretch film for palletised loads

Lore Gielkens

Scriptie ingediend tot het behalen van de graad van master in de industriële wetenschappen: chemie

PROMOTOR :
Prof. dr. Rosa PEETERS

PROMOTOR :
dr. ing. Bram BAMPS

Gezamenlijke opleiding UHasselt en KU Leuven

UHASSELT KU LEUVEN

Universiteit Hasselt | Campus Diepenbeek | Faculteit Industriële Ingenieurswetenschappen | Agoralaan Gebouw H - Gebouw B | BE 3590 Diepenbeek

Universiteit Hasselt | Campus Diepenbeek | Agoralaan Gebouw D | BE 3590 Diepenbeek
Universiteit Hasselt | Campus Hasselt | Martelarenlaan 42 | BE 3500 Hasselt

UHASSELT KU LEUVEN

2024
2025

Faculteit Industriële Ingenieurswetenschappen

master in de industriële wetenschappen: chemie

Masterthesis

Evaluating the impact of reprocessed content and multiple reprocessing cycles on the performance of polyethylene stretch film for palletised loads

Lore Gielkens

Scriptie ingediend tot het behalen van de graad van master in de industriële wetenschappen: chemie

PROMOTOR :

Prof. dr. Rosa PEETERS

PROMOTOR :

dr. ing. Bram BAMPS

UHASSELT KU LEUVEN

Preface

This Master's thesis is written within the Master's degree of Chemical Engineering Technology. The research conducted in this thesis investigates the effect of multiple reprocessing cycles and different amounts of reprocessed content on polyolefin stretch films' properties. This is a highly relevant topic in the present day, addressing the transition to a circular economy, a transition I would like to contribute to.

This work was completed within the MultiRec project, a CORNET-TETRA project that unites international research groups/institutes with the packaging industry. Research and tests were performed within the Materials and Packaging Research & Services group (MPR&S) of Hasselt University. I am grateful to have received the ISTA Student Research Grant for this research, which acknowledges the importance of researching pallet load stability during transport.

I would like to thank my promoter Prof. dr. Roos Peeters for her guidance and supervision, but also for giving me the opportunity to be awarded the ISTA Student Research Grant. I am thankful to my co-promoter dr. ing. Bram Bamps for his guidance and advice throughout the project, and for enhancing my understanding and perspectives. I would also like to thank Paula Varas Perez for her help performing the chemical tests and for helping me gain a better understanding of chemical analysis methods. Additionally, I am thankful to all the researchers in the MPR&S group who helped me with performing the tests of this research.

Finally, I would like to thank my friends and family for their support.

Contents

List of Tables

List of Figures

Glossary

Chain scission	The breaking of polymer chains during degradation.
Cross-linking	The formation of chemical bonds between polymer chains that connect them together, creating a three-dimensional network structure.
Pre-stretch	The stretching of the film during wrapping to improve load containment.
Machine direction (MD)	The direction parallel to film production flow.
Cross direction (CD)	The direction perpendicular to film production flow.
Biaxial orientation	The stretching of polymer chains in both machine and cross directions.
Polyolefin	A class of polymers including polyethylene and polypropylene, commonly used in plastic packaging.
Mono-material packaging	Packaging made from a single type of plastic material, facilitating easier recycling.
Load unitisation	The process of combining individual packages into a single, stable unit for handling and transport.
Tertiary packaging	Packaging used to group and protect secondary packages during transport and storage.
Long Chain Branching (LCB)	Refers to the presence of long side chains attached to the main polymer backbone during polymerisation.
Short Chain Branching (SCB)	Refers to a type of branching with short side chains.
Comonomer	Secondary monomer incorporated during polymerisation to modify polymer properties.
Bubble stability	The ability to maintain consistent bubble formation during blown film extrusion.
Bioaccumulation	The accumulation of substances in living organisms over time.
Tackifier	Additive that enhances adhesive properties but can accumulate on surfaces.
Green washing	Misleading marketing about environmental benefits of products.
Crystallinity	The degree in which atoms or molecules are ordered in a repeating pattern.
Amorphous region	A region where the polymers are randomly oriented.
Carbonyl index (CI)	A measure of degradation of a polymer based on the absorption of carbonyl groups in infrared spectra.
Molecular Weight Distribution (MWD)	The distribution of molecular mass within a polymer.

Abbreviations

ACC	Analytical and Circular Chemistry
ATR	Attenuated Total Reflection
BUVS	Benzotriazoles UV-Stabilisers
CD	Cross Direction
CI	Carbonyl Index
COF	Coefficient of friction
DSC	Differential Scanning Calorimetry
EU	European Union
FTIR	Fourier-Transform Infrared Spectroscopy
FTL	Full Truckload
GC-MS	Gas Chromatography-Mass Spectrometry
GPC	Gel Permeation Chromatography
HALS	Hindered Amine Light Stabilisers
HDPE	High Density Polyethylene
LCB	long chain branching
LDPE	Low Density Polyethylene
LLDPE	Linear Low Density Polyethylene
MD	Machine Direction
MFI	Melt Flow Index
MWD	Molecular Weight Distribution
PCR	Post Consumer Recycled
PDI	Polydispersity Index
PE	polyethylene
PIB	Polyisobutylene
PIR	Post Industrial Recycled

PPWR Packaging and Packaging Waste Regulation

rPE recycled polyethylene

rLLDPE reprocessed LLDPE

SAXS Small Angle X-ray Scattering

SCB short chain branching

SEC Size Exclusion Chromatography

SEM Scanning Electron Microscopy

ULDPE Ultra-Low Density Polyethylene

ULLDPE Ultra Linear Low Density Polyethylene

WAXS Wide Angle X-ray Scattering

XRD X-Ray diffraction

Abstract

Plastic packaging materials are essential for goods protection and during transport, but their environmental impact has prompted regulatory action. The EU's PPWR 2025/40 mandates 35% recycled content by 2030, rising to 65% by 2040. This Master's thesis investigates how reprocessed content and multiple reprocessing cycles affect LLDPE stretch film performance for palletised loads.

As part of the MultiRec project, this research evaluates films containing 0%, 35%, and 60% reprocessed LLDPE subjected to 5, 10, or 15 reprocessing cycles. The study examines mechanical properties, transport performance, UV-resistance, and seeks to interpret the findings based on chemical analysis.

Results show that chain scission is the dominant degradation mechanism, reducing polymer chain length and weakening polymer networks. While films maintained load stability in transport tests, mechanical performance decreased with increased reprocessing. Machine direction tear resistance showed the most pronounced degradation of mechanical properties, dropping from 5.3±0.35 N (virgin) to 0.70±0.14 N (15x60%). Another clear trend was the increase in permanent deformation and reduction in stress retention, indicating a loss of elasticity. The 15x60% film failed during wrapping at 100% pre-stretch due to gauge band defects. Surprisingly, UV-resistance improved with more reprocessing levels, likely due to increased HALS concentrations.

Findings suggest the EU's 2030 target appears achievable, the 2040 target needs advancements to overcome performance limitations.

Abstract in het Nederlands

Kunststofverpakkingen zijn essentieel voor productbescherming en transport, maar hun milieu-impact heeft tot nieuwe regelgeving geleid. De PPWR 2025/40 van de EU vereist 35% gerecycleerd materiaal tegen 2030, oplopend tot 65% in 2040. Deze masterscriptie onderzoekt hoe herwerkt materiaal en meerdere herwerkingscycli de prestaties van LLDPE rekfolie voor gepalletiseerde ladingen beïnvloeden.

Dit onderzoek evalueert folies met 0%, 35% en 60% herwerkt LLDPE na 5, 10 of 15 herwerkingscycli als onderdeel van het MultiRec-project. De studie analyseert mechanische eigenschappen, transportprestaties, UV-bestendigheid en interpreteert de bevindingen o.b.v. chemische analyse.

Resultaten tonen dat chain scission het dominante degradatiemechanisme is, waarbij polymeerketenlengte afneemt en netwerken verzwakken. Hoewel folies de palletstabiliteit behielden bij transporttesten, verslechterde de mechanische prestatie bij meer herwerking. Scheurweerstand in machinerichting toonde de meest uitgesproken degradatie van mechanische eigenschappen, dalend van 5.3±0.35 N (virgin) naar 0.70±0.14 N (15x60%). Een andere trend was de toename in permanente deformatie en afname in stressretentie, dat wijst op een verlies van elasticiteit. De 15x60% folie faalde tijdens wikkelen bij 100% voorrek vanwege gauge band defecten. Als verrassend resultaat verbeterde de UV-bestendigheid bij meer herwerking, mogelijk door verhoogde HALS-concentraties.

Bevindingen suggereren dat het EU-doel van 2030 haalbaar lijkt, maar het doel van 2040 vereist verdere ontwikkelingen.

Chapter 1

Introduction

1.1 Context

This Master's thesis, conducted in the MPR&S group, a research group within research institute Imo-Imomec of Hasselt University, is part of the international research project MultiRec. MultiRec is a CORNET-TETRA project that unites international research groups/institutes with the packaging industry [1]. Due to this partnership, knowledge developed in a laboratory setting can be translated into industrial applications, bridging the gap between applied research and real-world implementation. The project investigates the effect of multiple reprocessing cycles and different amounts of reprocessed content on polyolefin stretch films' properties and applications [1].

As the packaging industry is one of the most prominent plastic outlets, this project addresses a critical challenge in the circular economy. The growing environmental concerns in the world are attributed to a higher amount of plastic waste because of the increased production and usage of plastics. The European Union (EU) has established ambitious targets to tackle these environmental concerns through the Packaging and Packaging Waste Regulation (PPWR) 2025/40. This directive includes a design for recycling criteria by 2030 and an obligation of recyclability at scale by 2035 [2, 3]. The integration of reprocessed and recycled material into plastic packaging often impacts the characteristics and quality of the plastic films, making this research particularly relevant.

This thesis examines the incorporation of mechanically reprocessed polyethylene (PE) into non-food-grade mono-material films, such as Linear Low Density Polyethylene (LLDPE) stretch films. These stretch films are applied in pallet wrapping as industrial packaging and bundling applications of primary or secondary packaged packages [4]. Stretch films' mechanical properties, such as their high tear strength and dart impact strength, make them widely used as a load unitisation material [4].

This research evaluates films containing 0%, 35%, and 60% reprocessed LLDPE subjected to 5, 10, of 15 reprocessing cycles. The study examines mechanical properties, transport performance, UV-resistance, and seeks to interpret the findings based on chemical analysis. Chemical characteristics are measured outside the scope of this thesis to try and interpret the results achieved with the following tests. First, the mechanical characteristics of the films with reprocessed content are investigated as they have to achieve comparable performance with commercially available

virgin stretch films to be able to replace them. Second, during the transport simulation research the performance of stretch film with reprocessed content as a tertiary packaging film is investigated by looking at the impact of vibrations, compressions, and shock on palletised loads. Third, UV can accelerate material degradation. Therefore, UV-resistant properties of stretch films are important to investigate because they are often exposed to sunlight during transport or storage.

1.2 Problem statement and research questions

The current problem with commercial stretch film is that its composition does not comply with the new guidelines described in the PPWR [2, 3]. The amount of reprocessed content in these films is too low and must increase to conform with this directive. The increase in reprocessed content can influence the properties of the film and its performance as stretch film. This results in the following research question: **"What is the impact of reprocessed content and multiple reprocessing cycles on the performance of PE as stretch film for palletised loads?"**. The research question can be subdivided into sub-questions:

1. *What is the impact of reprocessed content and multiple reprocessing cycles on the mechanical characteristics of small-scale laboratory samples taken from stretch film intended for wrapping palletised loads?*
    - What is the impact of 35% and 60% reprocessed content on the mechanical characteristics of PE stretch film?
    - What is the impact of the number of reprocessing cycles (0, 5, 10, 15 cycles) on the mechanical characteristics of PE stretch film?
2. *What is the impact of reprocessed content and multiple reprocessing cycles on the performance of stretch film as transport packaging for palletised loads?*
    - How does 35% and 60% reprocessed content impact the performance of stretch film as transport packaging for palletised loads?
    - What is the impact of the number of reprocessing cycles (0, 5, 10, 15 cycles) on the performance of stretch film as transport packaging for palletised loads?
3. *What is the impact of reprocessed content and multiple reprocessing cycles in stretch films on the films' UV-resistance and the stretch films' performance of small-scale laboratory samples taken from stretch film intended for wrapping palletised loads?*
    - How does UV-light exposure influence PE stretch films' performance?
    - Does 35% and 60% reprocessed content influence the films' resistance to UV-light?
    - Does exposure to UV-light have a higher impact on stretch film performance with more reprocessed content?
    - Do 0, 5, 10, and 15 reprocessing cycles influence the films' resistance to UV-light?
    - Does exposure to UV-light have a higher impact on stretch film performance that contains reprocessed content with more reprocessing cycles?

1.3 Objectives

The primary objective of this Master's thesis is to evaluate how reprocessed content and multiple reprocessing cycles impact the PE stretch film's performance. The objective was aimed to be accomplished by the end of this project on the 20th of June by pursuing these sub-objectives:

- Characterising the mechanical properties of PE stretch films containing no reprocessed content (= virgin film, as reference), 35%, and 60% of reprocessed content, that has been reprocessed for 5, 10, or 15 cycles. This objective and its reporting were aimed to be completed by the first week of May.
- Assessing the transport performance characteristics of stretch films with no reprocessed content, 35%, and 60% of reprocessed content, that has been reprocessed for 5, 10, and 15 cycles, by conducting transport simulation tests. This goal was aimed to be completed and reported by the second week of May.
- Evaluating and reporting the impact of reprocessed content and multiple reprocessing cycles on the UV-resistance and stretch film performance after UV-light exposure by the first week of May through controlled UVA-light exposure testing with the analysis of chemical and mechanical properties after a certain exposure time.

1.4 Methods

The project was divided into different work packages to achieve the objectives described in the previous section. Each package contributed to one of the sub-objectives from the previous section.

Work package 1: Mechanical characterisation

The fundamental mechanical properties were assessed through standardised tests on small-scale laboratory samples. First, the tensile test (ISO 527-3 2018, ASTM D882 2002) determined stress and strain, by extending specimens along their longitudinal axis until failure [5, 6, 7]. Second, the puncture resistance was evaluated (ASTM F1306 2016, ASTM D5748) to assess the film's resistance to penetration of sharp edges [8, 9]. Additionally, the dart impact test was performed to determine resistance to impact (ASTM D1709 2003) [10].

Film-to-metal plate interactions were characterised through the coefficient of friction test (ISO 8295 2004, ASTM D1894) by measuring static and dynamic friction coefficients [11, 12]. Also, durability was assessed via the tear resistance test (ISO 6383-2 2004) [13]. Last, the film's elastic behaviour, including recovery from extension and stress retention, were evaluated (ASTM D5459) [14].

Work package 2: Transport simulation research

Transport performance was evaluated on unitised palletised loads using the ISTA 3E procedure [15]. This procedure tested the shipment performance of a Full Truckload (FTL) delivery. The test consisted of atmospheric preconditioning, atmospheric conditioning, a swing test and a tilt test, with an optional vibration pretreatment [15].

Work package 3: UV-light exposure (QUV)

QUV accelerated weathering tests exposed the specimens to cycles of 16 h of UVA-light, 15 min of water spray, and 3.75 h of condensation for 10 weeks (ISO 4892-1 2016, ISO 4892-3 2016) [16, 17]. Tensile and relaxation properties with small-scale laboratory samples were measured at different exposure times to evaluate degradation effects. The UV-degradation was assessed further through chemical analysis to explain the behaviour of the film after UV-light exposure.

Work package 4: Master's thesis writing

The research findings and methodology were documented throughout the project in this Master's thesis.

Work package 5: Communication

Project meetings to discuss experimental progress, analyse results, and address technical challenges were scheduled. Meetings with companies were scheduled on the 13th of March and the 26th of May, as well as meetings with project partners on the 26th of February and the 30th of April. These meetings ensured proper alignment with the research objectives and the timely completion of all other work packages.

1.5 Outlook

The following chapter examines the circular economy principles, stretch film consistencies and performance, and mechanical recycling methodologies.

The materials and methods section starts with an explanation of the materials used in this thesis, followed by a short explanation of the chemical characterisation methods. Next, the mechanical characterisation tests and the transport performance tests are explained in detail. Last, the methodology of the UV-resistance test is described.

The results of the study are presented in the results and discussion section. Finally, the last chapter includes the conclusions and recommendations for future research opportunities.

Chapter 2

Literature study

2.1 Introduction

This study aims to contribute to the development of more sustainable packaging solutions that meet both performance standards and regulatory requirements. In response to growing environmental concerns and the EU's PPWR 2025/40, the packaging industry faces a growing pressure to recycle materials and to incorporate recycled materials into their packaging. Stretch films, which play a crucial role in palletised load stabilisation and protection during transport, present a challenge. This literature study provides an understanding of the transition to a circular economy, stretch films, and mechanical recycling pathways. The study first addresses the transition to a circular economy. Next, the fundamental aspects of stretch films, including their application, composition, production process, and technical challenges are discussed. Furthermore, there is an emphasis on the mechanical recycling of PE. To evaluate the impact of recycled content and multiple recycling cycles, an overview of the methods of mechanical characterisation and transport simulation are presented.

2.2 Transition to a circular economy

2.2.1 Why is the transition to a circular economy important?

Our global economy follows a linear "take-make-dispose" model, shown in Figure 2.1(a), which contributes to climate change and environmental pollution by placing constant pressure on finite resources [18]. To address these challenges, there is a push to transform this linear economy into a circular one, where materials never become waste but are continuously recirculated through maintenance, reuse, refurbishment, remanufacturing, and recycling, illustrated in Figure 2.1(b) [19]. This "Butterfly Diagram" was developed by the Ellen MacArthur Foundation, which leads efforts to accelerate this transition [19]. Plastics exemplify the problems of our linear economy, despite their versatility and durability, over half are discarded after a single use [18]. According to StatBel, plastic packaging had a recycling rate of only 54% in 2022. This is significantly lower than other packaging materials, such as glass (98%), metal (96%), and paper and cardboard (86%) [20]. Their inconsistent disposal and resistance to degradation lead to fragmentation into micro and nano plastics that contaminate environments, food chains, and water bodies [18].

(a) Linear economy

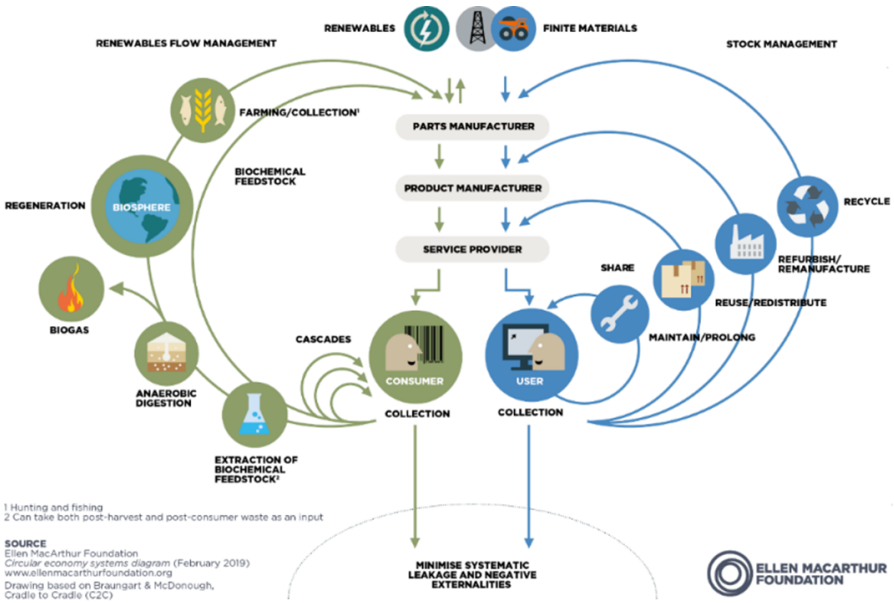

(b) Butterfly diagram of the circular economy of the Ellen MacArthur Foundation [19]

Figure 2.1: Transition to circular economy

2.2.2 What are the EU directives and regulations on packaging and packaging waste?

Recognising this problem, the EU has enforced guidelines and regulations, including Directive 94/62/EC on packaging and packaging waste [21]. This directive introduces taxes and mandates specific recycling rates. While the focus has been on developing alternative feedstocks to make plastics, these new materials can often not match the conventional plastics' low cost, performance characteristics, and scale of production. These limitations demonstrate the importance of a wide range of approaches that include promoting reuse, reducing plastic consumption, and encouraging recycling efforts. The directive specifically addresses these challenges by setting ambitious targets for packaging and packaging waste [21]. With its goal to increase the plastic packaging recycling rate from 55% to 70% by 2030, the directive highlights the prevention of packaging waste production. Apart from that, it also emphasises the promotion of various forms of material recovery, marking a notable step towards a circular economy [21].

Entering 2025, this directive has been replaced by the PPWR 2025/40 [2]. The goal of this regulation is to improve the environmental performance of packaging by introducing recyclability requirements for all packaging by January 2030 and recyclability at scale obligations from January 2035 [3]. Furthermore, it contains reuse and recycled content targets, as well as measures to prevent and reduce packaging waste generation [3]. The regulation mandates 35% of recycled content in packaging by 2030, rising to 65% by 2040. To achieve these targets and be conform these new regulations innovations in the plastic packaging industry are needed. Among various plastic products, stretch film presents unique challenges in the transition to more sustainable packaging solutions. Unlike many other plastic products, stretch film is not easy to maintain,

reuse or refurbish. This limitation makes that recycling is particularly interesting for this material. For that reason, understanding how recycled content and multiple recycling cycles affect the performance of PE stretch film for palletised loads becomes more and more essential for developing effective circular solutions. To understand this it is important to know its consistency and why it is so widely used.

2.3 Stretch film

2.3.1 What is the role and benefit of stretch film in load unitisation?

In the logistics sector, load utilisation is crucial for achieving multiple operational benefits, including reduced handling costs, enhanced product protection, and transport savings. Among the different load unitising methods, stretch film has emerged as one of the most popular choices [4]. The reason for its popularity is its combination of versatility, cost-effectiveness, protection capabilities, and productivity benefits. Some other advantages of the use of stretch film are its scan through optics, easy removal, and excellent protection against moisture, dirt, and abrasion [4]. Most of the properties that make stretch film popular are delivered by the primary material used in stretch films, PE. PE provides essential mechanical properties such as high tear strength, high elongation and tensile strength, as well as good self-adhesion and excellent transparency [22]. These characteristics make stretch film suitable as a secondary or tertiary packaging material for various applications, from building materials and car parts to chemicals, food products, and paper goods [22].

The effectiveness of stretch film lies in its application process. During the wrapping process, the film is stretched and afterwards it returns to nearly its original size [23]. This generates a tension, usually called containment force, that is strong enough to secure the load. The stretch wrapping process is usually enhanced by the use of corner boards, 90°-angle strips that can be made from various materials [23]. These corner boards provide additional support and stability.

Alternative load unitisation methods

Apart from stretch film there are alternative load unitising methods [24]. A fist alternative is **stretch hooding and shrink wrapping**. While operating on similar principles as traditional stretch film, stretch hooding uses a bag or hood that is stretched over the load before returning to nearly its original size. Similarly, shrink wrapping uses an oversized bag. However, instead of stretching, the bag is heated to make it shrink around the load. Both of these methods offer advantages through single-layer material use and five-sided load protection, making them suitable for outdoor storage [23]. **Strapping**, another alternative, uses plastic or metal bands to secure palletised loads. Plastic strapping is particularly advantageous due to its low material use, recovery characteristics, and elongation properties. It offers flexibility in application and different joining methods are available based on equipment and application needs. This solution is especially suitable for loads that do not require surface protection [23]. A third alternative is **mesh, roped pre-stretch film and vented film**. The food industry's needs, particularly for organic products requiring airflow during transport, has prompted the development of these specialised solutions as they provide varying degrees of breathability and load stability. Of these alternatives, roped pre-stretch film uniquely combines breathability with cost savings and optimal load security [24].

Sustainable innovations and their development challenges

The environmental crisis has driven development of sustainable solutions like paper-based load unitising. While developers claim paper wraps can reduce carbon footprints by up to 62% [25], their sustainability benefits remain questionable. Paper, though renewable, requires more expensive manufacturing and likely more material than plastic alternatives [26]. Additionally, technical limitations include poor structural integrity after tearing, below-standard wrapping speed, and limited water resistance [26]. These challenges highlight the short-term importance of researching plastic stretch films with higher recycled content and increased recycling cycles. This research requires comprehensive understanding of films' consistency, additives, manufacturing, wrapping techniques, and recycling methods that collectively affect performance.

2.3.2 What is stretch film made of?

To establish a thorough foundation for analysing stretch film performance, this section examines the composition and structural variations of PE. As mentioned before stretch film is most commonly made of PE because of its cost-effectiveness, excellent toughness and flexibility [5]. As shown in Figure 2.2(a) PE, a homopolymer composed of carbon and hydrogen atoms, exists in several variants, shown in Figure 2.2(b). This figure shows that these variations diverge in long chain branching (LCB) and short chain branching (SCB), Molecular Weight Distribution (MWD), crystallinity, comonomer and comonomer distribution [5, 27]. This chapter focuses primarily on LLDPE and Low Density Polyethylene (LDPE), as these are the dominant materials used in industrial stretch film applications. LLDPE serves as the primary polymer in most modern stretch films, while LDPE is sometimes incorporated as a processing aid and property modifier. Other PE variants fall outside the scope of this discussion due to their limited relevance to stretch film manufacturing.

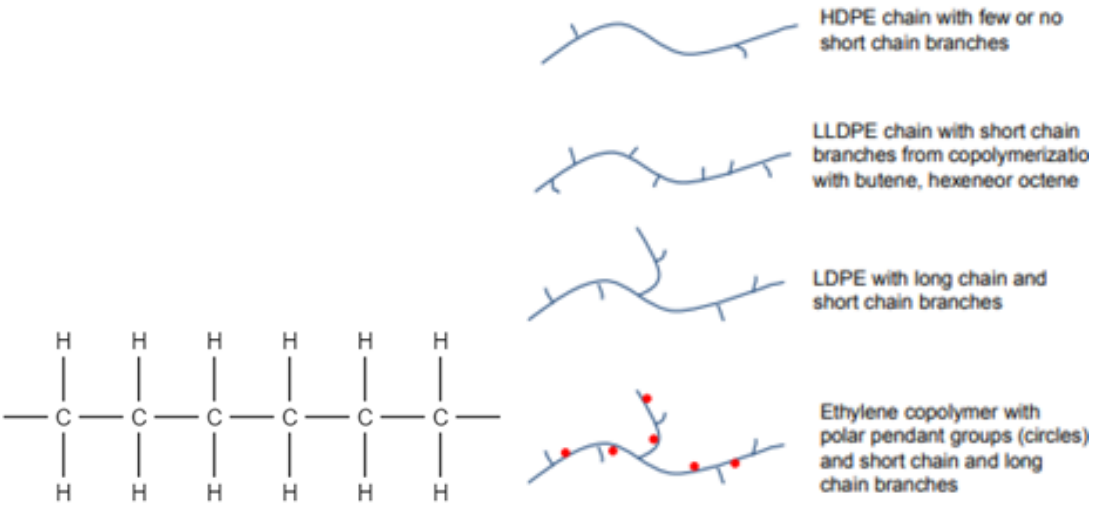

(a) Structure of PE (b) PE structure differences [5]

Figure 2.2: PE structure

Linear low density polyethylene (LLDPE)

LLDPE is characterised by predominantly linear chains with minimal LCB [27]. With a density range of 0.90-0.94 g/cc [5], LLDPE's density is controlled by comonomer incorporation during polymerisation, utilising butene, hexene, or octene as non-polar comonomers [5, 28]. Higher comonomer content increases SCB, while disrupting crystallinity and lowering density. The comonomer size determines short chain branch length, which impacts the final film properties [5]. LLDPE production employs coordination catalyst processes using three main catalyst types [5, 29]. Figure 2.3 illustrates the structural differences between polymers produced using Ziegler-Natta catalysts versus metallocene catalysts.

- Chrome-based catalysts produce LLDPE with very broad MWD [29].
- Ziegler-Natta catalysts generate a wide MWD and usually a greater amount of comonomer can be found on the shorter chains. As a result, there will be long chains that show High Density Polyethylene (HDPE)-like behaviour because of their lack of short chains and comonomer [30].
- Metallocene catalysts provide a more tightly controlled MWD and comonomer distribution. Therefore, the polymer will have improved properties including a higher tear strength, lower melting point and seal initiation temperature, a higher impact toughness and hot tack strength, greater clarity, and fewer extractables [31, 32].

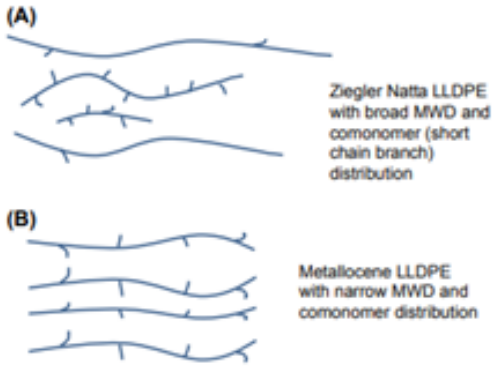

Figure 2.3: Different chain structure of (A) Ziegler-Natta and (B) metallocene catalysed LLDPE [5]

The properties of LLDPE are influenced by several parameters: comonomer content, comonomer type, catalyst type, and production process. LLDPE's versatility makes it integral to flexible packaging applications, serving as a sealant, providing bulk and structural support, and functioning as a tie resin component [5]. LLDPE proves to be superior for pallet load unitisation due to its enhanced mechanical properties, specifically its higher tear strength, superior dart impact resistance, and greater flexibility. These characteristics are essential for effectively securing and protecting palletised goods during storage and transportation.

On the contrary, LDPE is synthesised via free radical polymerisation in high-pressure environments and has a similar density range (0.92-0.94 g/cc) [5]. While LDPE offers better blown film bubble stability and processing characteristics due to its LCB, LLDPE generally demonstrates superior dart impact resistance, ultimate seal strength, and tear strength [5, 27, 33]. LDPE often serves as a complementary material in LLDPE applications, used as a blending additive to reduce haze and enhance processability in blown films.

2.3.3 What additives are used in stretch film?

Environmental factors and surface contaminants can diminish the film's performance. The incorporation of additives into the LLDPE matrix enhances the stability, functionality, and performance of these films. By adding these additives, such as antioxidants and UV-stabilisers, their application potential can expand across diverse industrial contexts [5].

Antioxidants

Weathering resistance is crucial for stretch films, particularly when used for loads stored outdoors. Environmental factors such as UV-light, thermal oxidation, humidity, and temperature variations can alter the film's mechanical properties and cause aesthetic deterioration, such as discolouration [34]. Oxidative degradation, also known as autoxidation, includes induced formation of free radicals, leading to modifications in the macromolecular structure via cross-linking or chain scissions. During initiation, a free radical from the hydrocarbon chain or an excited oxygen extracts a hydrogen atom [34]. Consequently, an organic radical forms that reacts with oxygen to produce polymer hydroperoxides. As a result, the molecular structure and molar mass of the polymer changes due to the hydroperoxides and their decomposition products [34].

Addition of proper stabilising additives, called antioxidants, can inhibit the oxidative degradation in polymers. Antioxidants are chemical compounds that protect against thermal and photo-oxidative processes [34, 35]. They can be categorised into two groups based on their mechanism. Primary antioxidants, also known as chain-breaking antioxidants, function through chain-breaking electron donor mechanisms to scavenge free radicals [35]. The inhibition of the oxidation takes place through chain termination reactions. Primary antioxidants include H-donors (sterically hindered phenols, secondary aromatic amines) and radical scavengers [34, 35]. Secondary antioxidants, or hydroperoxide decomposers, break down hydroperoxides with the formation of inert secondary products [35]. These are often used in combination with primary antioxidants [34]. The combination of both will result in synergetic stabilisation effects. Common examples include phosphites, phosphorus compounds, and thiosynergists [35].

Recent developments have introduced multifunctional antioxidants, which combine several stabilising functions in single molecules. These simplify formulation, storage, handling, and usage while eliminating the need for co-stabilisers [35]. A common primary antioxidant in stretch films is Irganox® 1076, often used with co-stabiliser Irgafos® 168 [36, 37].

UV-stabilisers

PE's sensitivity to UV-degradation necessitates protection during transport and outdoor storage of loads unitised with PE stretch film [34, 35]. UV-exposure triggers an oxidative chain-radical reaction, forming product like carboxylic acids, aldehydes, and ketones that affect mechanical and aesthetic properties [38]. This process is often called photo-degradation. UV-stabilisers, added in soluble and active form at concentrations of 0.01 to 1.0 wt%, seek to prevent UV-absorption of the polymer but also to prevent the antioxidants from photo-degrading [38]. Hindered Amine Light Stabilisers (HALS) such as Tinuvin® 622, Chimassorb® 944, and CGL 116 are commonly used [39, 40].

Other types of UV-light stabilisers are Benzotriazoles UV-Stabilisers (BUVS). These organic ultraviolet absorbers absorb UV-rays and release energy as longer wavelengths or heat, without changing their own physicochemical properties [41]. More particularly, BUVSs are often used because of their wide absorption wavelength range (300-385 nm). Due to their bioaccumulation and toxicity their use will be withdrawn [41].

Cling agents

For stretch film applications, LLDPE with octene comonomer types can be used. These films can achieve bonding between two non-polar PE films due to primary mechanical adhesion [42]. The mechanical adhesion is facilitated by van der Waals forces and molecular chain entanglements. However, high pre-stretch can reduce cling effectiveness by increasing side chain orientation on the film surface causing difficulties when interacting with each other. Polyisobutylene (PIB) serves as a cling agent to enhance cling force regardless of pre-stretch levels [42, 43]. When added to the PE matrix, PIB forms two phases due to incompatibility. PIB is being distributed within the amorphous phase and migrates to the film surface to enhance cling properties [42, 43]. Use of mono-materials is one of the strategies in the transition of plastics to a circular economy. This is why research is being executed on the use of Ultra-Low Density Polyethylene (ULDPE) as a cling agent in the outer layer leading to a higher quality recycled material.

Other additives

Stretch films' low electrical conductivity and hydrophobicity make them prone to surface electrical charge accumulation, limiting their use in packaging static-sensitive electronics. Traditional amphiphilic surfactant **antistatic agents** provide temporary solutions due to disappearance from the surface [44]. Alternative approaches include conductive fillers like graphene [45], carbon nanotubes [46], and carbon black [47]. More recent research shows interest in quaternary ammonium salt-based copolymers, as they have an enhanced polarity and charge density. However, difficulties with compatibility are limiting its use. Due to its very specific application, antistatic agents are not commonly used in stretch film [48]. During processing and use of stretch film, the coefficient of friction is an essential property. While low friction facilitates processing, higher friction can reduce the required number of film layers [49]. **Slip additives**, such as erucamide and oleamide, are commonly used to modify this coefficient of friction [50]. They are added to the polymer matrix in molten state and migrate to the film surface upon solidification due to incompatibility with the film matrix [51]. Their use in stretch film is rare due to the undesirable migration of the slip agents to the surface of the film. Use of **colourants** in stretch films is limited, only white colourants are occasionally employed to enhance UV-resistance. The use of colourants is generally discouraged as they complicate the recycling processes.

2.3.4 How is stretch film made?

Stretch film production employs various manufacturing methods. The most used manufacturing method is extrusion, it starts with conversing PE pellets into melted plastic [4]. These pellets are fed into the extruder's hopper funnel and dropped into the barrel where they are heated to their melting point. A continuously rotating screw pushes the molten material through the barrel. The melted polymer is subsequently forced through the extruder die and shaped to form a plastic film [4].

For more complex applications, co-extrusion can be used [4]. It enables the production of multi-layered stretch films by extrusion with multiple dies and extrudates to create films with distinct layer compositions and properties. Following the initial extrusion phase, the manufacturing process diverges into two distinct methods [4]. **Cast film** production involves forcing the extruded plastic through a slit-shaped die [4, 33, 52]. The plastic sheet that comes out of the slit-shaped die is pulled vertically downward between rollers, which orientates the polymer molecules predominantly in the Machine Direction (MD) [33]. The film is then cooled through chilled rolls and precisely dimensioned through cutting operations [4, 52, 53]. Alternatively, **blown film** fabrication uses a round die to form the extrudate into a continuous hollow tube [4, 33, 52]. This tube is inflated with air and blown vertically upward, creating biaxial orientation of the polymer chains in both MD and Cross Direction (CD) [33]. After cooling, the tube is flattened, cut, and wound into rolls for distribution [4, 52, 53].

Each manufacturing approach offers specific advantages. Cast extrusion delivers higher production speeds and efficiency, while blown film extrusion produces films with superior strength characteristics due to enhanced polymer orientation in both MD and CD [4]. For palletised load applications, where higher levels of orientation are not critical, cast film extrusion is typically preferred for its production efficiency. Figure 2.4 displays the cast and blown film extrusion processes.

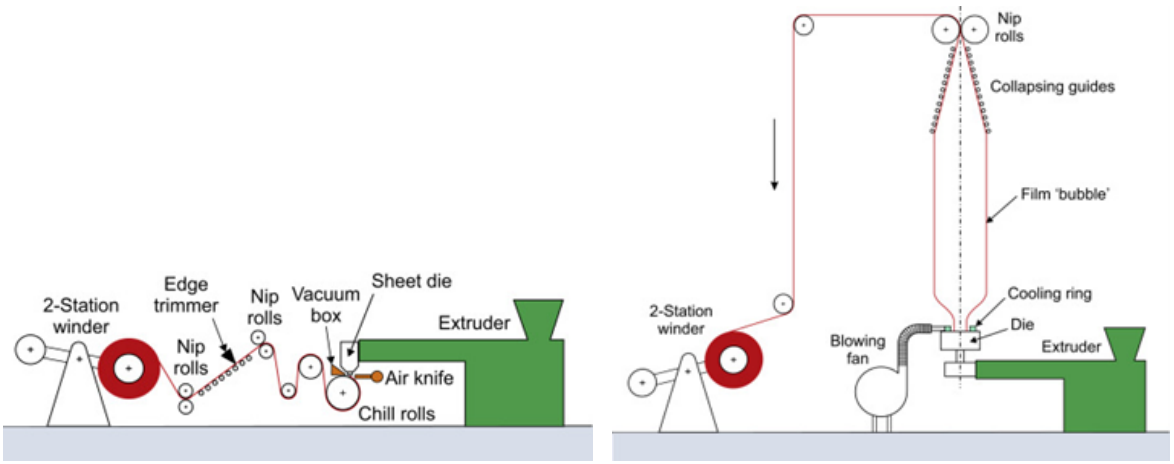

(a) Cast film extrusion [53]

(b) Blown film extrusion [53]

Figure 2.4: Film extrusion processes

2.3.5 How are stretch films wrapped?

During the stretch wrapping process and subsequent transport and storage phases, containment force emerges as a critical factor in maintaining load integrity. This force is essential for keeping the load components securely unified [23]. The balance of containment force requires precise calibration: excessive force may result in product damage, while insufficient force can lead to load failure. The appropriate containment force varies based on several load characteristics, including weight, height, and column strength [23].

The evolution of stretch-wrap machinery began with the wide-web model, which used large rolls of stretch film. As the demand to wrap variable pallet load heights grew, manufacturers developed the spiral model employing smaller film rolls. This innovation enabled the film roll to traverse vertically, wrapping the load in an efficient criss-cross pattern [54]. Two different configurations of spiral wrappers exist. On one hand, there is a turntable that spins the pallet while the film roll moves vertically up and down. On the other hand, there is a spiral wrapper which moves the roll completely around the pallet while the pallet itself stays still. Currently, the spiral wrappers, available in both semi-automatic and fully automatic configurations, dominate the industrial wrapping machinery sector. For operations with different requirements or constraints, hand wrapper models provide an alternative wrapping solution [54].

The operational sequence of the wrapping process commences with positioning the load on the stretch wrapper's turntable. Upon activation, the turntable starts rotating, while drawing film from the designated supply roll [54]. Before the application of the stretch film to the load, pre-stretch is created. This is accomplished through a pre-stretch assembly, which extends the film by routing it between two powered rolls. This pre-stretch process significantly reduces the cost per pallet load by minimising the material consumption [54]. During wrapping a secondary stretch is created as well, resulting in different wrapping scenarios. A low secondary stretch can be used to cause a relaxation of the film on the pallet resulting in a lower containment force. Alternatively, a high secondary stretch leads to further stretch of the film on the pallet generating a higher containment force. The secondary stretch can help with applying the pre-stretch as consistent as possible when it is set at the right value.

The stacking of the boxes on the pallet can have an influence on the wrapping process and load stability as well. Possible configurations are load-on-load stacking and load-between-load stacking [55]. Load-on-load stacking, also known as column stacking, is fast and easy, and results in maximum utilisation of the pallet space. However, it is less stable and only applicable on uniform loads. Load-between-load stacking, or interlocking stacking, provides more stability and safety, and is applicable for irregular loads. However, it needs more skill and experience, it is slower, and it results in less efficient use of space on the pallet [56].

2.3.6 What are the challenges when using stretch films?

Challenges of stretch film

It is important to apply proper handling of stretch film to prevent edge damage and maintain optimal performance. Various manufacturing defects, illustrated in Figure 2.5 may compromise film quality, including the presence of gels, black specks, tail-overwind issues, scalloped edges, gauge bands, roll telescoping, and feathered edges [4]. **Gels** are places with a high molecular weight or with unmelted polymer and can be seen as clear, hard and round spots. Next, **black specs** are caused by foreign material resulting in film imperfections and degraded polymer. **Tails-overwind** can be described as disrupted material by transfer onto the winder. Additionally, **scalloped edges** are a result of poor slitting which generating sawtooth-appearing edges. **Gauge bands** are gauge variations that cause soft or hard rings on the roll. Furthermore, **roll telescoping** is created by sliding of layers of the film, increasing the roll width. **Feathered edges** are layers of film that extend past the end of the film roll. Users frequently encounter operational challenges such as film breakage, tail management difficulties, and tackifier accumulation on surfaces.

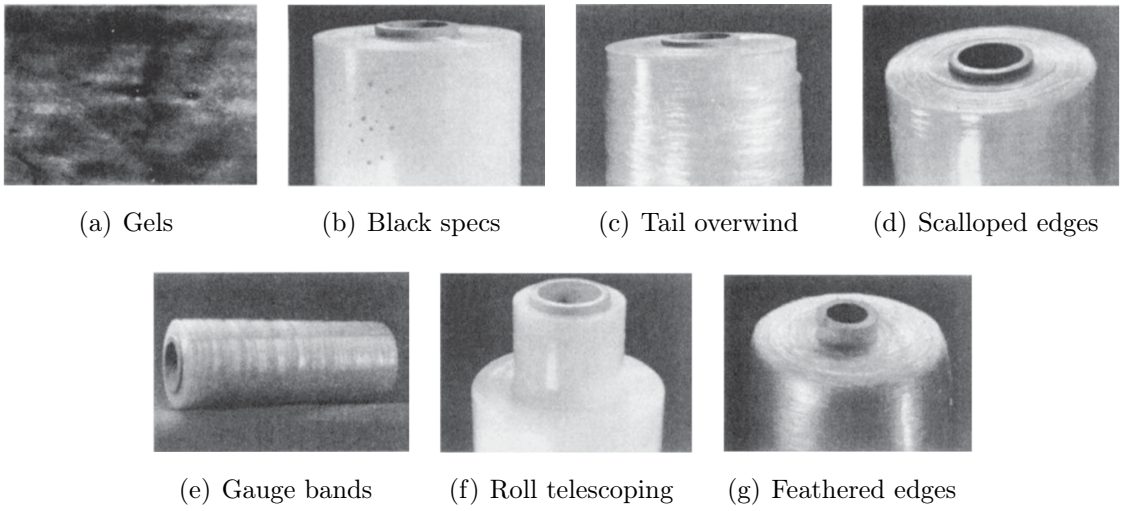

(a) Gels (b) Black specs (c) Tail overwind (d) Scalloped edges

(e) Gauge bands (f) Roll telescoping (g) Feathered edges

Figure 2.5: Manufacturing defects of stretch film rolls [4]

Environmental factors significantly influence stretch film performance throughout its service life. External storage exposes the film to potential photo-degradation from UV-radiation, degrading both mechanical properties and visual appearance as mentioned before. Temperature fluctuations can substantially alter the film's characteristics, affecting elasticity, tensile strength, and cling properties. When used to package electronic components, static discharge presents a notable risk, potentially damaging sensitive devices contained within the film. Surface contaminants such as dust and grit particles can compromise the film's adhesive qualities and diminish its overall performance capabilities. Additionally, excessive vertical stacking of palletised loads creates redundant pressure on lower packages, which can deform both the film and the protected goods [4].

Challenges of Post Consumer Recycled (PCR) stretch film

The incorporation of PCR materials introduces significant processing challenges due to elevated contaminant levels and material inconsistency. Comprehensive knowledge of PCR resin specifications becomes crucial before initiating production processes [57]. These inherent impurities and variability inevitably impact the film's performance. One of their limitations is their inability to achieve the industry-standard 200% pre-stretch [57]. Further complications are the potential presence of unidentified additives within PCR materials, which may affect performance parameters. Apart from the difference in processability and performance, PCR usually also shows aesthetical differences, such as a less transparent film, potentially affecting customer acceptance of the final product [57].

2.3.7 Which stretch films are commercially available?

There are various kinds of stretch film commercially available, such as, pre-stretch film, hand stretch film, and bundling film. These films come in different sizes usually ranging from 250 mm to 500 mm and different stretchabilities ranging from 120% to 300% elongation. PCR films are already commercially available as well, containing different percentages of PCR ranging from 30% to 80% recycled content. However, it is often difficult to trace the origin of the PCR material that is used and how much is actually used. Sometimes it is not necessarily PCR but Post

Industrial Recycled (PIR) material that is used in the films, which is a way of green washing when called PCR material. New developments of chemical analysis methods are important to determine whether or not green washing takes place. The films are usually made from PE using cast film extrusion and commonly contain three layers, however the number of layers can also be more than three. Different film thicknesses are available as well, ranging from 17 to 35 μm. The price of the films is dependent on the type of pallet and load and is determined by the maximum carrying capacity that is needed for the load. The price of machine wrap films usually varies from 60.00 to 110.00 euros per roll, depending on the properties and performance. Hand wrap films are usually cheaper, they cost around 10.00 to 20.00 euros per roll, however these rolls are usually smaller because they cannot be as heavy as the machine films. There are a large number of suppliers, examples are Rajapack®, Coeman®, and Darco® [58, 59, 60].

2.4 Mechanical recycling of PE

2.4.1 Which recycling methods are available?

Recycling creates a closed loop system that generates secondary "raw materials". These materials can be achieved through either mechanical or chemical recycling processes. Mechanical recycling yields granulates, while chemical recycling breaks down the material into monomer building blocks [61]. The different types of recycling methods can be classified according to their material quality preservation. Primary recycling produces materials with equal or improved properties compared to virgin materials. Secondary recycling (mechanical recycling) results in materials with diminished properties compared to the virgin material. Tertiary recycling (chemical recycling) breaks down plastics into monomers or chemical products. Quaternary recycling refers to plastic energy recovery through incineration, though in a circular economy this is not considered true recycling [61]. Mechanical recycling is prioritised over chemical recycling in the circular economy due to its lower energy requirements and reduced environmental impact. A schematic representation of the recycling methods is presented in Figure 2.6 [61].

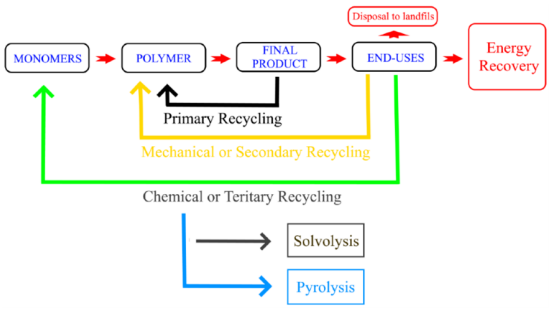

Figure 2.6: Schematic representation of recycling methods [61]

Recycling can also be classified on the basis of the end products created from the secondary raw material [61]. On one hand, closed-loop recycling reincorporates recycled materials into the same product categories they came from. On the other hand, open-loop recycling utilises recycled materials in applications different from their original products. The recycling of LLDPE can be seen as closed-loop recycling, because these films are often collected separately from other waste streams [61]. As a result, the secondary material can be used to make the same product as the product they came from.

2.4.2 How is stretch film recycled?

The mechanical recycling process for LLDPE stretch film typically follows several key steps. Initially, LLDPE stretch films are collected separately from other plastic waste streams, significantly simplifying the sorting process. The collected films then undergo initial sorting, shredding, washing, secondary sorting, and extrusion [61, 62]. After recycling, the pellets are blended with virgin LLDPE to maintain the critical properties required for stretch film applications. Figure 2.7 shows an example of a mechanical recycling process. Despite its advantages, current mechanical recycling technologies face limitations related to processing costs, degradation of mechanical properties, and inconsistent quality in the final recycled materials. These challenges underscore the importance of waste reduction strategies alongside recycling improvements, as minimising solid plastic waste production remains a critical environmental objective.

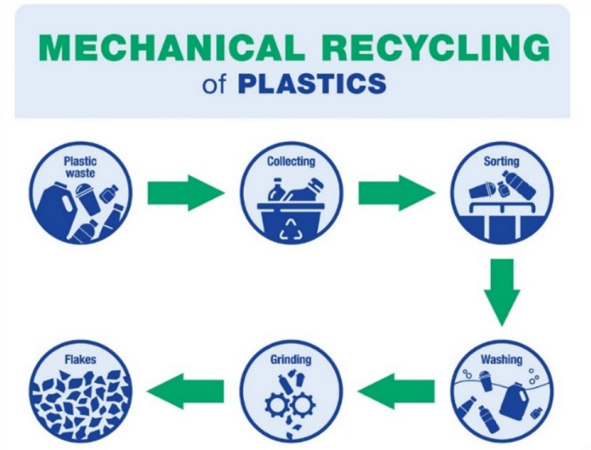

Figure 2.7: Example of mechanical recycling process [63]

2.5 Possible test methods for stretch film

2.5.1 Mechanical characterisation methods

There are a lot of different properties that are typical for flexible packaging [4]. Each of these properties can be tested with a certain test method. Table 2.1 shows the different properties that can be tested with their standard test method [4, 5]. By testing these properties according to their standard test method, the different types of stretch films can be compared in mechanical characteristics. Each of these characteristics can be tested separately but to get a better idea of the film's performance a FPT-750 film performance tester can be used. This tester simulates real-world application conditions, enabling integrated puncture testing, cling force measurement, relaxation testing, and film consistency evaluation during wrapping [17].

2.5.2 Transport simulations testing

Stretch film for unitised loads requires testing through transport simulations, with ISTA procedure 3E being commonly used to evaluate full truckload delivery performance [15]. This is done through a series of atmospheric conditioning, shock tests, compression, vibration, and edge drop tests. Alternative methods include EUMOS 40509 2020 stability test using horizontal acceleration and the tilt test at a 26° angle [64].

Table 2.1: Mechanical characterisation methods [5]

ASTM method	**Property**	**Importance**
D792	Density	Cost, layer control
D3418	Melt temperature	Seal initiation temperature, extrusion temperature
E1356	Glass transition temperature	Melt process, when material becomes brittle
D3418	Freezing temperature	Quench speed in converting process
D1525	Vicat softening temperature	Indication temperature resistance
D1238	Melt flow rate	Flowability in polymer process
Various	Viscosity	Processing characteristics
D882-2002	Tensile	Mechanical strength (ISO 527-3 2018)
F1306-2016 D5748	Puncture resistance	Slow rate penetration resistance
D1894	Coefficient of friction	Sliding and starting friction (ISO 8295 2004)
/	Tear resistance	Force needed to cut film (ISO 6383-2 2004)
/	Abrasion resistance	Ability to withstand wear (ISO 9352 2012)
D5459	Elastic recovery	Quantity of recovery and permanent deformation
D5458	Peel or cling	Cling between two layers of film

2.6 Conclusion

This literature study examined the transition of stretch films to a circular economy, with mechanical recycling as the most feasible pathway. The challenges posed by the EU's PPWR 2025/40 regulations were addressed as well. The packaging industry faces the dual challenge of enhancing sustainability while preserving critical performance attributes.

The stretch films can have different consistencies. The films are usually made of LLDPE using different production processes. A combination of LLDPE with different types of PE and additives is possible to enhance the performance of the films. However, one of the focusses in the transition of the plastic industry is the use of mono-materials, as they facilitate the recycling process. These films face multiple challenges such as manufacturing defects, degradation due to environmental factors, and incorporation of PCR material into the films.

LLDPE stretch films undergo a mechanical recycling process that involves collection, sorting, shredding, washing, and extrusion. The mechanical recycling creates secondary raw materials with diminished properties compared to virgin materials. This results in challenges such as property degradation and quality inconsistencies that highlight the importance of further research.

Chapter 3

Materials and methods

3.1 Materials

3.1.1 Raw material

The raw material, used to make the films, consists of 100% quasi-unadditivated LLDPE with a density of 0.918 g/cc. This material has a Melt Flow Index (MFI) of 2.0 g/10 min, a molecular weight of 240 357 g/mol, a dispersity of 4.49, and a melting temperature of 123.4°C. The raw material already contains primary (Irganox® 1076) and secondary (Weston® 705) antioxidants, and no further supplementation is done. The raw material was additivated with 2000 ppm of oligomeric HALS. Another material that is added in the inner layer, to increase cling properties, is Ultra Linear Low Density Polyethylene (ULLDPE). ULLDPE has a density of 0.904 g/cc and a MFI of 4 g/10 min.

3.1.2 Stretch film

Commercial reference films

The virgin film of brand A, consists of 3 layers of LLDPE that were cast co-extruded. The film has a width of 500 mm and a thickness of 23 μm. The PCR film of brand A consisted of 30% post consumer waste. The anti-UV film of brand A has a resistance of 12 months. The virgin film of brand B has a width of 500 mm and a thickness of 23 μm. The PCR film of brand B has the same dimensions and contains 30% PCR. There are also two UV-resistant films one with 6 months of resistance (25 μm thickness) and one with 12 months of resistance (28 μm thickness).

Laboratory films

The laboratory stretch films consist of a simple ABC structure and are co-extruded, using cast extrusion, during the manufacturing process. The main components of the films are virgin and reprocessed LLDPE. The inner layer (layer A) consists of 50% virgin LLDPE and 50% ULLDPE. The core layer (layer B), includes a percentage of virgin LLDPE and a percentage of reprocessed LLDPE (rLLDPE). The different percentages of materials for layer B are shown in Table 3.1. The outer layer (layer C), is composed of only virgin LLDPE. The layer structure can be seen in Figure 3.1.

Table 3.1: Layer B configurations

		Reprocessed content		
		0%	**35%**	**60%**
Reprocessing cycles	0	X		
	5		X	X
	10		X	X
	15		X	X

Figure 3.1: Layer structure of lab films

3.2 Methods

3.2.1 Conditioning

The films were conditioned at 23 ± 2°C and 50 ± 10% relative humidity for at least 24 h before testing, following ISO 291:2008. Conditioning during transport tests depended more on outside weather conditions, so temperature and relative humidity were recorded during each transport test.

3.2.2 Chemical characterisation methods

All chemical characterisation methods were performed by researchers of the MPR&S research group outside the scope of this thesis. The equipment used for these tests was provided by the Analytical and Circular Chemistry (ACC) research group.

Differential Scanning Calorimetry (DSC)

The different films were analysed using a DSC Q200 (TA Instruments, USA) at 10°C/min, 5–185°C (second heating cycle). These DSC measurements were employed to estimate the temperatures associated with melting (T_m) and crystallisation (T_c), as well as the enthalpy of fusion (ΔH_m). The crystallinity of the material was calculated using Equation 3.1.

$$X_c = (\Delta H_m / \Delta H_{100}) \cdot 100\% \tag{3.1}$$

Where

ΔH_m is the melting enthalpy;
X_c is the degree of crystallinity;
ΔH_{100} is the melting enthalpy of 100% crystalline ($\Delta H_{100} = 288 J/g$).

Gel Permeation Chromatography (GPC)

Size Exclusion Chromatography (SEC) was used to estimate the polymer molar mass distributions, performed at 160°C on an Agilent 1260 Infinity II high-temperature GPC. Polystyrene internal standards were used in combination with 1,2,4-trichlorobenzene as the eluent, and a PL-GEL 10 μm MIXED-B column.

Fourier-Transform Infrared Spectroscopy (FTIR)

The effect of photo-oxidation on the films has been studied by monitoring the evolution of carbonyl groups. Attenuated Total Reflection (ATR)-FTIR was performed on both sides of the initial film and on the samples after UV-exposure. Spectra were collected employing an Invenio S (Bruker, Germany) equipped with a Platinum ATR accessory. FTIR data were acquired in the mid-IR region (4000-400 cm^{-1}) with 64 scans co-added at a spectral resolution of 4 cm^{-1}. Before spectral acquisition of each sample, 64 background scans were collected. Data was processed using QUASAR software. To measure the evolution of carbonyl groups during thermal or photo-degradation the Carbonyl Index (CI) is determined. It is the ratio of the integrated absorbance band correlating the carbonyl group (1850-1650) to the absorbance band of the methylene scissoring (1500-1420). Atmospheric effects are taken into account by taking the integral from the baseline after correcting the data [65].

Gas Chromatography-Mass Spectrometry (GC-MS)

GC-MS following Soxhlet extraction was used to screen the additives. Intact film samples (5 g) were extracted for more than 5 h using 300 ml of 50:50 hexane:dichloromethane solution. Analysis was performed on a Trace 1310 gas chromatograph (Thermo Scientific) with a DB-5MS capillary column (30 m length, 0.25 mm I.D., and 0.25 μm film thickness, Agilent Technologies USA) coupled to an ISQ LT single quadrupole mass spectrometer (Thermo Scientific, USA). Injection conditions were 1 μL sample volume with 1/100 split and the injection port was set at a temperature of 280°C. The oven temperature program had an initial temperature of 50°C and ramped to 330°C at 15°C/min, with a final hold of 9 min. The mass spectrometer conditions were the following; electron ionisation (70 eV), 250°C source temperature, 50-700 m/z range, 0.1 s scan time, 280°C transfer line, and helium carrier gas at 1.2 ml/min. Data processing used Chromeleon 7.3.

3.2.3 Mechanical characterisation methods

Thickness measurement

The film thickness was measured according to ASTM D698 using a WOLF Messtechnik GmbH device. Ten random measurements were taken across each film sample, avoiding the edges because they can be thicker. Mean thickness and standard deviation were calculated for each film. Figure 3.2 shows the measuring device.

Figure 3.2: WOLF Messtechnik GmbH thickness measurer

Coefficient of friction (COF)

The COF was determined using ISO 8295 standard with a horizontal test table, made of non-ferromagnetic metal, and a sled attached to an MTS 10/M tensile tester using a 10 N load cell. The sled, with a surface of 40 cm^2 and an edge length of 63 mm, weighed 200 ± 2 g. The sled exerted a normal force of 1.96 ± 0.02 N with a uniform pressure distribution due to the elastic base of the sled. The test was conducted at a speed of 100 ± 10 mm/min, measuring both inside and outside film surfaces against the metal test table, with five repetitions. The specimens were placed on the test table with test side facing down, and the sled positioned centrally on top of the specimen. Ten seconds after the test was started, the sled started moving to measure the static and dynamic frictional forces. Test set-up is shown in Figure 3.3.

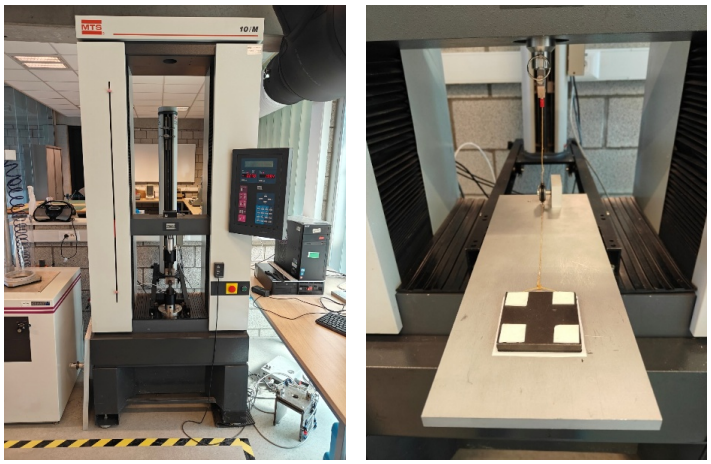

(a) MTS tensile tester (b) Set-up

Figure 3.3: COF test

The determination of the static COF is done by determining the static frictional force. The static frictional force, F_s, is the maximum point of the force that increases linearly. The static COF is then given by Equation 3.2.

$$\mu_s = F_s/F_p \tag{3.2}$$

Where

F_s is the static frictional force, expressed in newtons (N);
F_p is the normal force exerted by the mass of the sled, expressed in newtons (= 1.96 N).

The dynamic COF is the average force over the first 6 cm of movement after the start of the relative movement between the surfaces in contact. The static force peak was neglected while determining the dynamic COF. The dynamic frictional force was then calculated using Equation 3.3.

$$\mu_D = F_D/F_p \tag{3.3}$$

Where

F_D is the dynamic frictional force, expressed in newtons;
F_p is the normal force exerted by the mass of the sled, expressed in newtons (= 1.96 N).

Tensile test

The tensile test was conducted according to standards ISO 527-1 2019, ISO 527-3 2018, and ASTM D882 2002 using a Tinius Olsen Horizon 5ST machine with Horizon software. Rectangular specimens of 15 mm width and at least 150 mm length were tested in MD at 1500 mm/min with 0.20 N preload and a gauge length of 20 mm. Five specimens were tested per film type. The tensile test set-up and machine can be seen in Figure 3.4. After starting the test, the specimen was extended at a speed of 1500 mm/min in MD until break. During the test the following parameters were measured: force (N), time (s) and position (mm).

(a) Tensile test set-up (b) Tensile test machine Tinius Olsen

Figure 3.4: Tensile test

The measured parameters could be used to determine the stress (at break), strain (at break), and the Young's Modulus. For each of these variables the mean and standard deviation were determined for each film type. The stress σ (MPa) could be calculated using Equation 3.4.

$$\sigma = F/A_0 \tag{3.4}$$

Where

σ is the stress, in MPa;
F is the measured force, in N;
A is the initial cross-sectional area of the specimen, in mm^2.

The stress at break, σ_{break} (MPa), was calculated at the moment of fracture with Equation 3.5.

$$\sigma_{break} = F_{break}/A \tag{3.5}$$

The elongation, ΔL (mm), is the absolute increase in length of the material calculated using Equation 3.6. In contrary, the strain ϵ (%) is the normalised elongation and describes the relative deformation and could be calculated using Equation 3.7.

$$\Delta L = L_c - L_0 \tag{3.6}$$

$$\epsilon = \Delta L/L_0 = (L_c - L_0)/L_0 \tag{3.7}$$

Where

ϵ is the strain value, in %;
L_0 is the initial gauge length of the test specimen, in mm;
ΔL is the increase of the specimen length, in mm.

The strain at break, ϵ_{break} (%), is how much a material deforms before it fractures and is given by Equation 3.8.

$$\epsilon_{break} = (L_{break} - L_0)/L_0 \tag{3.8}$$

The Young's Modulus, E (MPa), can be determined as well, however for stretch film it is not an accurate modulus, as it is only valid in the elastic region which is a very small proportion of the curve. The Young's Modulus could be determined with Equation 3.9.

$$E = \sigma/\epsilon \tag{3.9}$$

Stress-relaxation test

The stress-relaxation test utilised the Tinius Olsen 5ST tensile tester with Horizon software and follows standard ASTM D5459-95. The films were subjected to elongations of 200%, 300%, and 400% (typical pre-stretch levels for machine wrapped films) to determine recovery from extension, stress retention, and permanent deformation. Additionally, stress-relaxation tests were conducted at 38 ± 1°C and 60 ± 1°C to assess temperature effects on elastic properties. Samples were conditioned in the Tinius Olsen's oven for 5 min at the corresponding test temperature before testing.

Five rectangular samples with a width of 15 mm were cut in MD for each film. The samples were clamped at 25 mm grip separation and elongated at a speed of 127 mm/min to their target elongation (curve AB in Figure 3.5). The samples were held at this elongation for 1 min inducing relaxation (curve BG), then returned to the original clamp separation and held for 3 min (curve GCA), before being re-extended to the original elongation (curve ADX). The mean and standard deviation of each of the following parameters was calculated.

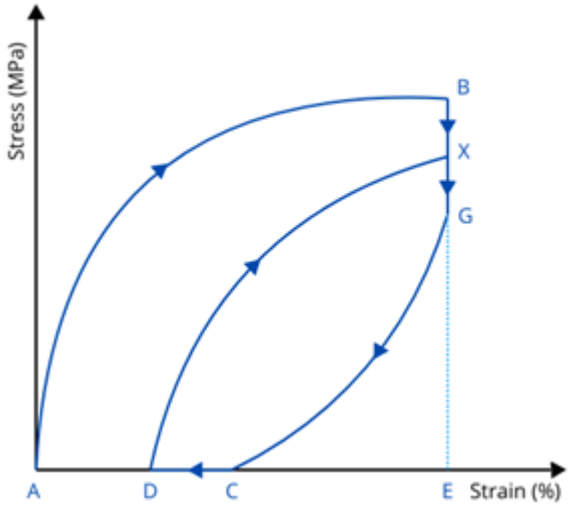

Figure 3.5: Example graph of relaxation test

The permanent deformation, PD (%), was calculated using Equation 3.10 with the length of AD and AE of Figure 3.5.

$$PD = (AD/AE) \cdot 100 \tag{3.10}$$

With the length of DE and AE the elastic recovery, ER (%), could be calculated with the use of Equation 3.11.

$$ER = (DE/AE) \cdot 100 \tag{3.11}$$

By determining the length of BE and GE and the use of Equation 3.12, the stress retention, SR (%), could be calculated.

$$SR = (GE/BE) \cdot 100 \tag{3.12}$$

Slow rate penetration test

The slow rate penetration test followed ASTM F1306-16 to determine the film's resistance to a driven probe. This is a more general characterisation method. To simulate puncture conditions on pallets more accurately, the film should ideally be tested in a pre-stretch state. However, this is technically not feasible with current testing equipment. Square specimens of 76 mm by 76 mm were tested five times per film type until perforation. Direction (MD or CD) was irrelevant due to biaxial stress application. The samples were clamped in the machine's bottom head. Testing began at 10 mm/min until detection of a preload of 0.20 N, at this preload the speed increased to 25 mm/min and penetrated until puncture. Measurements included ultimate force (UF), probe penetration depth (PP) and energy to break (EB), calculated using Equation 3.13. The experimental set-up can be seen in Figure 3.6.

$$EB = UF \cdot PP \cdot 0.001 \tag{3.13}$$

(a) Slow rate penetration test (b) Slow rate penetration set-up

Figure 3.6: Slow rate penetration test

Tear resistance test

The tear resistance test followed ISO 6383-2 2004 to determine the force required to tear the film specimens using an Elmendorf type MTS ED30 machine shown in Figure 3.7(a). The tear resistance is the force required to tear a specimen by this method. This test should ideally be tested in pre-stretched conditions as well, but testing equipment limits the possibility. Constant-radius specimens, displayed in Figure 3.7(b), were prepared using a sample cutter, visible in Figure 3.7(c) and Figure 3.7(d), to avoid edge defects. The film thickness was measured before testing. For both MD and CD, five specimens sampled evenly across the film were tested. Preliminary tests ensured the pendulum energy absorption remained between 20-80% of the total capacity. One weight was added when testing CD samples to maintain this range. Specimens were clamped in the machine before releasing the pendulum. Mean force (N) and standard deviation were calculated from the measurements.

(a) MTS ED30 Elmendorf tear resistance tester

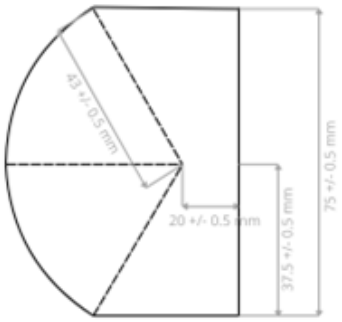

(b) Constant radius specimen

(c) Constant radius sample cutter

(d) Sample cutter

Figure 3.7: Tear resistance test

Dart impact test

The dart impact test followed ASTM D1709 2003 to determine film failure energy under free-falling dart impact. The test used a Ceast tester with a 38.10 ± 0.13 mm dart dropped from 0.66 ± 0.01 m height, visible in Figure 3.8. The specimens extended beyond clamp gaskets, using full film width with measurements distributed along the length of the films.

Figure 3.8: Ceast dart impact tester

Testing employed the staircase technique with 15 g weight increments. The film was clamped followed by the release of the dart. Films were examined for fails, fails occurred if any breakthrough was visible. After each test, weight was decreased by 15 g if the film failed or increased by 15 g if the film did not fail. The same method was employed until a total of 20 tests was reached. If the number of failed tests was equal to 10 the test was complete. However, if the number of failed tests was lower than 10, the test was continued until 10 failed test were reached. If the number of failed test was higher than 10, testing continued until 10 not failed tests were completed. The total number of failed tests was reported as n_i, counting only the last 10 failures. The lowest failure-causing weight was assigned $i = 0$, with subsequent weights numbered sequentially (1, 2, 3...). The product of n_i and i was calculated as in_i. Finally, the impact failure weight (W_f) was determined using Equation 3.14.

$$W_f = W_0 + [\Delta W \cdot (A/N - 1/2)] \tag{3.14}$$

Where

N is the sum of all n_i's (in this test always = 10);
A is the sum of all in_i's;
W_0 is the dart weight to which an i value of 0 was assigned (g);
ΔW is the uniform dart weight increment (15 g).

3.2.4 Transport simulation test methods

Pallet preparation

To prepare the pallet that is used for the transport simulation tests one EUR-pallet with the dimensions of 0.800 m by 1.20 m was used. Additionally, double-wall corrugated cardboard boxes (Cad53a of Rajapack®) were used measuring 0.4 m by 0.3 m by 0.3 m. The boxes needed a recommended shipping density of 192 kg/m^3 according to ASTM D4169. Resulting in boxes filled with ± 6.2 kg of granulate per box. Additionally, cardboard edge protectors type CRN357 of Rajapack® were used. The boxes were stacked in a six layer column stacking configuration to achieve the highest possible challenge for the stretch film, as the column stacking configuration can lead to blooming effects.

Wrapping process

The pallet is wrapped with the different types of film using the Coeman Spinny S350 automatic wrapper which is displayed in Figure 3.9(a). The rotation speed of the wrapper was set at 75% with an up and down speed of 20 and a film tension of 18. The pallet was wrapped seven times at the base layer and three times at the top layer to decrease horizontal displacement, determined by performing preliminary tests outside the scope of this thesis by two MPR&S researchers. The goal of the wrapping protocol was to achieve equal primary and secondary stretch. The pre-stretch of the wrapper was set at 100% because preliminary tests showed that films with 15 times reprocessed material could not be wrapped at higher pre-stretches. The film with 15x60% reprocessed material even failed the wrapping test at 100% pre-stretch due to tearing of the film at weak points. To be able to compare the results of the transport simulation tests, all other films were wrapped at 100% pre-stretch, as this was the maximum achievable pre-stretch possible.

Tilt test

The tilt test is performed to analyse load stability. The wrapped pallet was attached to the lifting system on one side. Next, the load was inclined to an angle of 26° and held there for 1 min. During the testing period the load's deformation was monitored. When no significant deformation was visible the pallet passed the test and when visible deformation appeared the pallet failed the test. The lifting system and a pallet during a tilt test can be seen in Figure 3.9(b).

(a) Coeman Spinny S350 wrapper

(b) Tilt test

Figure 3.9: Transport simulation tests

Swing test

The swing test is done to simulate a worse-case horizontal shock scenario using the set-up that can be seen in Figure 3.10(a) of Plakoni, Belgium. The set-up consists of a hinge mechanism of 280 cm, allowing the load to swing freely, and a pull-back distance before impact of 64 cm. The swing test was performed according to the ISTA Procedure 3E 2009. The collision generated by the test results in an acceleration force of 24 g. Tracker software was used for a video analysis to monitor the tilting of the load during the test. The video of the swing test was imported in this tracker software and the frame range was set so that the first 3 s of the test were analysed. Before analysis a calibration stick was added to the height of the loaded pallet (measuring 180 cm). Next, point masses were assigned to the middle of the top and bottom layer boxes. Finally, a reference point mass was assigned to a fixed spot on the swing to cancel out abnormalities. A picture of the tracker software analysis is shown in Figure 3.10(b). The data achieved by this analysis was processed to extract the tilting of the bottom and top layer of the films when subjected to the swing test.

The pallets without pretreatment, were tested 10 min after wrapping. The horizontal displacement was measured manually, by measuring the distance between the boxes and the wall before and after the test. Each film type was wrapped and subjected to a normal swing test. Additionally, each film type was wrapped and subjected to a vibrational pretreatment followed by the same swing test. More specifically, a random vibration pattern was applied with an overall G_{rms} level of 0.54, according to the ISTA 3E Procedure. The vibration spectrum is shown in Figure 3.10(c).

(a) Horizontal shock test or swing test Plakoni

(b) Tracker software analysis

(c) ISTA 3E Procedure random vibration spectrum

Figure 3.10: Swing test

3.2.5 UV-light exposure with QUV-tester

The QUV conditioning was determined according to ISO 4892-1 2016 and ISO 4892-3 2016. The films were cut into pieces of 30 cm and attached to the plates of the QUV-machine. Two films per plate were put into the QUV-machine with UVA-lamps. The machine that was used and an example of the plate with samples are displayed in Figure 3.11. In the machine the films go through a cycle of 16 h of light exposure followed by 15 min of water spray and 3.75 h of condensation. The UV-light exposure is tested on the outside of the films as they are exposed directly to UV-light during storage and transport. The samples were tested by chemical and mechanical characterisation at different exposure times. The mechanical characterisation consisted of a normal tensile test and a stress-relaxation test at 200% elongation, described in 3.2.3. The chemical characterisation included an FTIR and DSC measurement described in 3.2.2. The test was performed on the virgin film, the films with 5 times reprocessed material with both 35% and 60% recycled content, and the film with 10 and 15 times reprocessed material with 60% recycled content.

(a) QUV-chamber

(b) QUV plate with film samples

Figure 3.11: QUV-machine and set-up

Chapter 4

Results and discussion

The results and discussion are presented in two main sections. First, material characterisation of the films progresses from chemical characterisation at the molecular scale, to mechanical properties assessment on laboratory samples, and finally transport simulation at pallet scale. Second, the impact of UV-exposure is examined through changes in chemical properties followed by effects on mechanical performance.

4.1 Material characterisation

4.1.1 Chemical analysis

The thermal properties of the stretch films were characterised using DSC to assess the impact of mechanical recycling on the material's crystalline structure and thermal transitions. The results of these tests are shown in Figure 4.1 and Table 4.1.

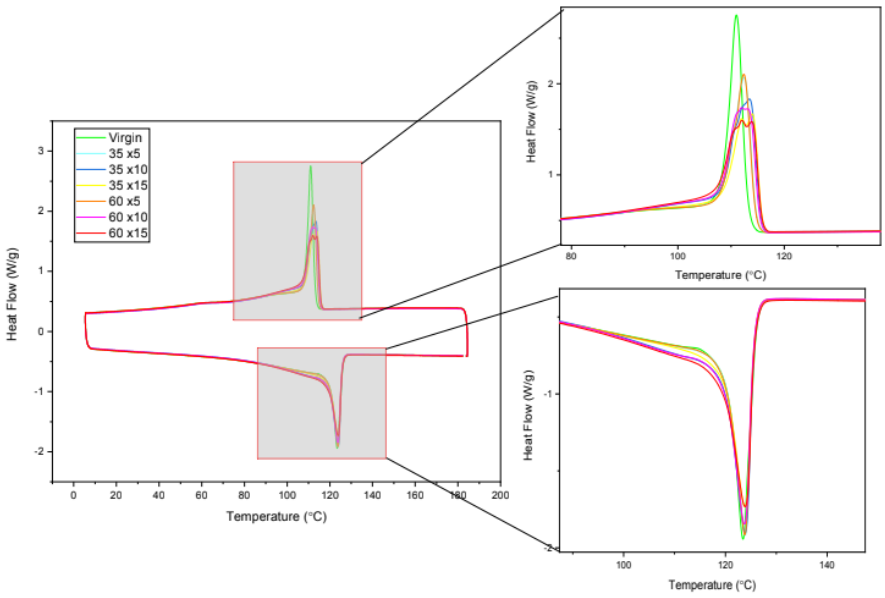

Figure 4.1: Results DSC lab films

Table 4.1: Results crystallisation temperature DSC lab films

	Virgin	5x		10x		15x	
		35%	60%	35%	60%	35%	60%
Tc (°C)	110.99	112.69	112.65	113.75	111.95	114.32	112.05

These results show a slight increase in crystallisation temperature (T_c) with increased reprocessing cycles. The films with 35% of reprocessed content show a higher T_c than the virgin film and the films with 60% reprocessed content. The temperature measurement of the DSC machine has a margin of error of 0.1 °C. The DSC tests that were performed on granulate samples show a slightly more clear increase in T_c going from 110.73°C to 114.20°C. However, the tests were performed only once on the different samples, limiting the statistical reliability of these comparisons and making it difficult to draw definitive conclusions about the effect of reprocessing on crystallisation temperature.

GPC tests performed on 1, 5, 10, and 15 times reprocessed granulate are visible in Table 4.2. Table 4.2 shows the number average molecular weight (M_n), the weight average molecular weight (M_w), and the dispersity (Đ) for the different numbers of reprocessing cycles.

Table 4.2: Results GPC of reprocessed granulate

	1x	5x	10x	15x
M_n (g/mol)	47308.0	48614.0	41321.0	31394.0
M_w (g/mol)	238757	230334	217072	228621
Đ	5.04686	4.73802	5.25331	7.28232

After 10 and 15 times reprocessing the M_n shows a clear decrease, pointing to more smaller chains as a result of chain scission. The dispersity increases as a result of the larger number of smaller chains in combination with a fewer number of large chains, making the MWD increase.

GC-MS results show a clear decrease in primary antioxidant depletion (Irganox® 1706) when the number of reprocessing cycles is increased. The primary antioxidant depletion decreases from 821 μg/g for granulate that is reprocessed one time to 74 mug/g for 15 times reprocessed granulate. The depletion of secondary antioxidants (HALS) is still under investigation.

4.1.2 Mechanical characterisation

Thickness measurement

Film thickness was measured across all samples as a critical parameter for normalising subsequent mechanical test results. Thickness influences the mechanical response and must be accounted for to enable meaningful comparisons between samples. The results of the thickness measurement of the lab films are displayed in Table 4.3. The thicknesses of the commercial reference films that were measured are demonstrated in Table 4.4.

Table 4.3: Result thickness measurement lab films

	Virgin	**5x**		**10x**		**15x**	
		35%	60%	35%	60%	35%	60%
Mean (mm)	**0.0299**	**0.0280**	**0.0268**	**0.0238**	**0.0268**	**0.0206**	**0.0164**
StDev (mm)	0.00156	0.00289	0.00197	0.00134	0.00301	0.00268	0.00140

Table 4.4: Result thickness measurement commercial reference films

	Brand A			**Brand B**			
	Virgin	PCR	UV12	Virgin	PCR	UV6	UV12
Mean (mm)	**0.0223**	**0.0236**	**0.0220**	**0.0232**	**0.0224**	**0.0246**	**0.0273**
StDev (mm)	0.000643	0.00145	0.000855	0.000803	0.00249	0.000793	0.00109

The thickness of the films lays between 0.0164 ± 0.00140 mm and 0.299 ± 0.00156 mm. The results show that the thickness of the worst case film is the lowest. The differences in thickness of the films is possibly a result of the difference in MFI of the films. The MFI shows the same trend of decreasing with reprocessed content and reprocessing cycles, going from around 7.8 g/10 min to 1.6 g/10 min. These MFI results were attained by tests performed by project partner Fraunhofer-IVV, with samples of 10 kg. The commercial stretch films have a thickness between 0.0220 ± 0.000855 mm and 0.0273 ± 0.00109 mm. The thickness of the lab films are comparable to the thicknesses of commercially available stretch films.

Coefficient of friction (COF)

The COF test was conducted to evaluate the surface properties and sliding behaviour of the stretch films under different contact conditions. This measurement is critical for stretch film applications, as friction properties influence winding behaviour, cling performance, and load stability. Table 4.5 displays the results of the COF test between the inside of the film and a metal plate as well as the outside of the films and the metal plate. Table 4.6 shows the results of the same test performed on the commercial reference films.

Table 4.5: Results COF test lab films

			Virgin	**5x**		**10x**		**15x**	
				35%	60%	35%	60%	35%	60%
Inside	Static	**Mean**	**0.427**	**0.452**	**0.358**	**0.416**	**0.403**	**0.458**	**0.452**
		StDev	0.0985	0.0301	0.0339	0.0196	0.00807	0.00559	0.0172
	Dynamic	**Mean**	**0.384**	**0.431**	**0.308**	**0.416**	**0.414**	**0.485**	**0.441**
		StDev	0.0680	0.0366	0.0310	0.0193	0.00989	0.0202	0.00331
Outside	Static	**Mean**	**0.418**	**0.406**	**0.344**	**0.428**	**0.412**	**0.441**	**0.448**
		StDev	0.0609	0.0423	0.0636	0.0226	0.00665	0.0172	0.00913
	Dynamic	**Mean**	**0.382**	**0.380**	**0.309**	**0.424**	**0.426**	**0.456**	**0.432**
		StDev	0.0395	0.0505	0.0595	0.0237	0.0210	0.0184	0.0140

Table 4.6: Results COF test commercial reference films

			Brand A		**Brand B**	
			Virgin	PCR	Virgin	PCR
Inside	Static	**Mean**	**0.450**	**0.654**	**0.447**	**0.452**
		StDev	0.0283	0.0259	0.0283	0.0099
	Dynamic	**Mean**	**0.472**	**0.619**	**0.479**	**0.487**
		StDev	0.0113	0.0179	0.0181	0.0098
Outside	Static	**Mean**	**0.556**	**0.579**	**0.535**	**0.469**
		StDev	0.0488	0.0301	0.0305	0.0295
	Dynamic	**Mean**	**0.503**	**0.504**	**0.502**	**0.447**
		StDev	0.0267	0.0165	0.0124	0.0310

When comparing the results of the insides of the films with the outsides, there is no significant difference in static COF, when the standard deviation is taken into account. The dynamic COF also shows no significant difference between inside and outside. For the insides of the films the most significant result is that the static and dynamic COF of the 5x60% film are lowest and the static and dynamic COF of the 15x35% film are highest. When comparing the other results there are no differences that are statistically meaningful. This is an expected result as the outer layer of each of these films is composed of the same virgin polymer. In comparison with the commercial reference films the lab films show a slightly lower static and dynamic COF on the inside as well as on the outside. This is possibly due to a difference in the polymers that are used in the outer layers of the films.

Tensile test

Tensile testing was performed to evaluate how repeated reprocessing cycles and varying reprocessed content levels affect the films' load-bearing capacity and deformation behaviour under MD stress conditions. The results that were achieved by performing the tensile test on the lab films are demonstrated in Figure 4.2(a). The results of the tensile test performed on the commercial reference films, performed by a coworker, are shown in Figure 4.2(b).

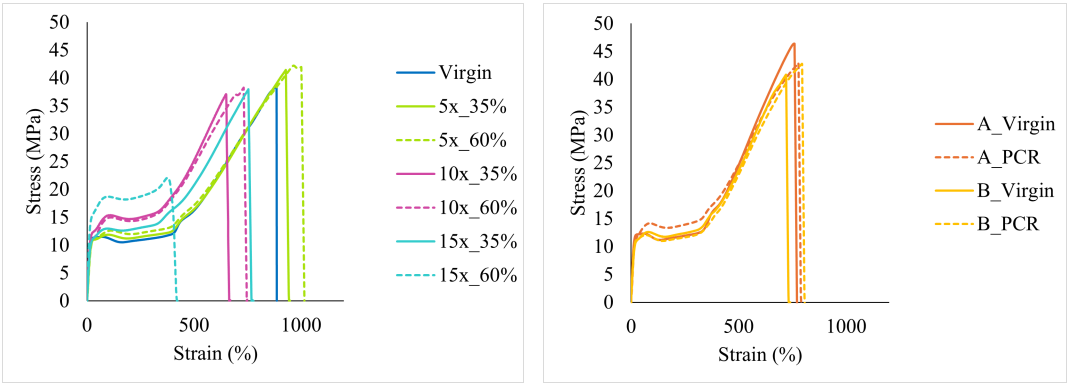

(a) Results tensile test lab films

(b) Results tensile test commercial reference films

Figure 4.2: Results tensile test

The tensile results in Figure 4.2(a) show that the **tensile stress at break** (σ_{break}) is 34.4 ± 1.99 MPa for virgin lab film. The films with 5 times reprocessed content show that the σ_{break} increases slightly for both numbers of reprocessed content (35% and 60%) to 42.8 ± 2.72 MPa and 39.5 ± 5.88 MPa respectively. The σ_{break} of the films with 10 times reprocessed content and the film with 15x35% reprocessed content lowers in comparison to the films with 5 times reprocessed content, more specifically to 37.2 ± 8.86 MPa for 35% reprocessed content and 38.4 ± 3.59 MPa for 60% reprocessed content. However, the tensile stress at break shows the most significant decrease for the 15x60% worst case film. When looking at the **elongation at break** (ϵ_{break}), for the virgin film (918 ± 29.3%), 5x35% (997 ± 76.5%), and 5x60% (910 ± 95.5%) times reprocessed films, there is no significant difference. This indicates that moderate reprocessing does not impair elongation performance. However, a slight reduction in elongation at break was observed for films with 10x35% (707 ± 150%), 10x60% (754 ± 84.9%), and 15x35% (822 ± 129%) reprocessed content. The reduction became more pronounced for the film with 60% of 15 times reprocessed content with a ϵ_{break} of 507 ± 161%. For the commercial reference films the σ_{break} has a mean of 43.47 ± 2.807 MPa, the ϵ_{break} has a mean of 747.7 ± 35.99% and the strain hardening starts at 300% strain. These results show clear similarities with the results of the lab films, visible in Figure 4.2. This means that the lab films and the commercial reference films have comparable tensile properties for the films with moderate reprocessing cycles.

Extended reprocessing appears to decrease the tensile properties of the films. However, high standard deviations in 10 times and 15x35% reprocessed films make this trend questionable. Only the film with 15x60% reprocessed content shows obviously weaker tensile properties, which points to a decrease of performance when a high number of reprocessing cycles is combined with a high amount of reprocessed content. This decrease is possibly due to changes in molecular structure, which are discussed more in detail in 4.1.4.

Stress-relaxation test

Stress-relaxation testing was conducted to evaluate the hysteresis loop of the stretch films under constant strain conditions. This test measures the time-dependent decrease in stress when a material is held at a fixed deformation. The stress-relaxation behaviour is particularly relevant for stretch film applications, where the material must maintain wrapping tension over extended periods. The results of the stress-relaxation test at different temperatures and different elongations are displayed in Table 4.7, Table 4.8, Table 4.9, Table 4.10 and Figure 4.3.

Table 4.7: Results stress-relaxation test lab films at 23°C

			Virgin	**5x**		**10x**		**15x**	
				35%	60%	35%	60%	35%	60%
200%	PD (%)	**Mean**	**50.12**	**48.85**	**48.30**	**52.53**	**53.19**	**52.50**	**54.62**
		StDev	0.6374	0.4242	0.4145	0.3157	0.4867	0.4667	0.4545
	SR (%)	**Mean**	**74.15**	**72.42**	**71.48**	**70.90**	**68.99**	**69.82**	**68.56**
		StDev	0.3775	0.2610	0.3486	0.8456	0.6289	0.1838	0.5188
300%	PD (%)	**Mean**	**63.91**	**63.83**	**64.57**	**67.62**	**67.79**	**67.50**	**69.12**
		StDev	0.3394	0.05804	0.2612	0.2972	0.2711	0.2012	0.5014
	SR (%)	**Mean**	**72.30**	**70.44**	**68.65**	**67.79**	**66.52**	**67.58**	**66.01**
		StDev	0.3554	0.4181	0.5281	0.2711	0.7031	0.7027	0.6434
400%	PD (%)	**Mean**	**74.21**	**74.80**	**75.14**	**77.38**	**77.29**	**76.78**	**77.90**
		StDev	0.2309	0.5213	0.3446	0.3295	0.2039	0.2475	0.1716
	SR (%)	**Mean**	**67.45**	**66.43**	**65.53**	**63.69**	**64.08**	**65.11**	**64.46**
		StDev	0.4105	0.4104	0.2522	2.807	0.7415	0.2488	0.4469

Table 4.8: Results stress-relaxation test lab films at 38°C

			Virgin	**5x**		**10x**		**15x**	
				5x35%	5x60%	10x35%	10x60%	15x35%	15x60%
200%	PD (%)	**Mean**	**50.60**	**49.59**	**48.89**	**52.85**	**52.61**	**51.59**	**54.38**
		StDev	0.2875	0.3813	0.8988	0.8459	0.4096	0.6293	0.4255
	SR (%)	**Mean**	**76.03**	**74.74**	**73.98**	**71.54**	**71.34**	**72.53**	**71.28**
		StDev	0.5022	0.3914	0.3952	0.5136	0.5647	0.5344	0.5686
300%	PD (%)	**Mean**	**65.70**	**65.04**	**65.61**				
		StDev	0.4862	0.7107	0.2529				
	SR (%)	**Mean**	**73.07**	**72.32**	**70.98**				
		StDev	0.7078	0.3643	0.2290				
400%	PD (%)	**Mean**	**74.00**	**74.11**	**74.54**				
		StDev	0.1723	0.2224	0.3970				
	SR (%)	**Mean**	**70.46**	**69.19**	**68.11**				
		StDev	0.6224	0.5694	0.3256				

Table 4.9: Results stress-relaxation test lab films at 60°C

			Virgin	5x		10x		15x	
				5x35%	5x60%	10x35%	10x60%	15x35%	15x60%
200%	PD (%)	**Mean**	**47.42**	**48.58**	**48.50**	**50.79**	**50.72**	**50.27**	**53.26**
		StDev	1.218	0.2976	0.8869	0.2652	0.6204	0.7181	3.362
	SR (%)	**Mean**	**78.51**	**76.82**	**76.49**	**75.64**	**74.93**	**76.13**	**75.34**
		StDev	0.2796	1.113	0.3779	0.5148	0.6948	0.2950	1.327
300%	PD (%)	**Mean**	**63.82**	**63.66**	**63.81**				
		StDev	0.3316	0.5288	0.3210				
	SR (%)	**Mean**	**76.12**	**74.25**	**73.78**				
		StDev	0.4513	0.5955	0.7478				
400%	PD (%)	**Mean**	**67.24**	**68.33**	**65.60**				
		StDev	0.7756	3.873	4.568				
	SR (%)	**Mean**	**74.68**	**71.32**	**71.60**				
		StDev	0.7899	2.035	0.4153				

Table 4.10: Results stress-relaxation test commercial reference films at 23°C

			Brand A		Brand B	
			Virgin	PCR	Virgin	PCR
200%	PD (%)	**Mean**	**55.70**	**69.42**	**69.45**	**66.61**
		StDev	1.325	1.345	0.3103	0.4123
	SR (%)	**Mean**	**72.24**	**67.47**	**69.40**	**70.41**
		StDev	0.6376	0.6034	0.7093	0.5809

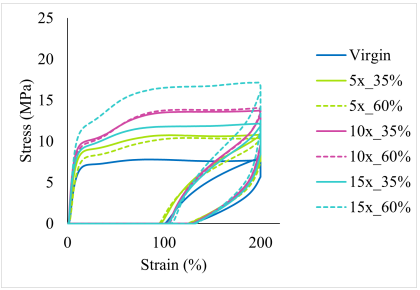

(a) Lab films: 23°C, 200%

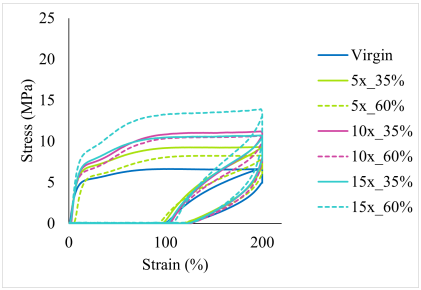

(b) Lab films: 38°C, 200%

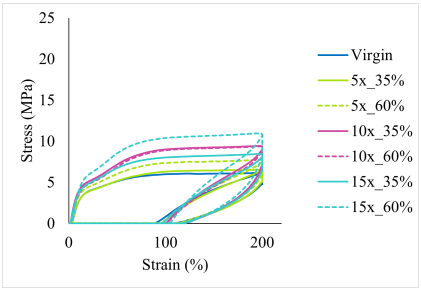

(c) Lab films: 60°C, 200%

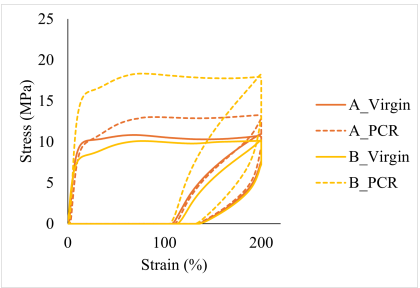

(d) Commercial reference: 23°C, 200%

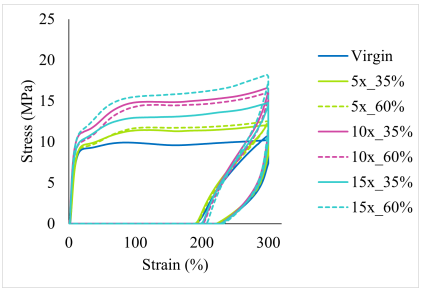

(e) Lab films: 23°C, 300%

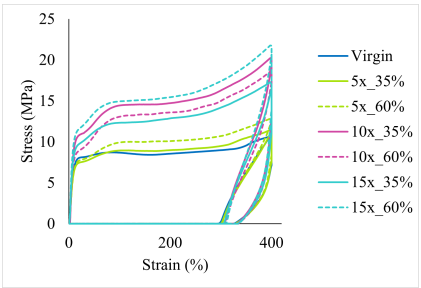

(f) Lab films: 23°C, 400%

Figure 4.3: Results stress-relaxation test at different temperatures and different elongations

Figure 4.3(a), Figure 4.3(e), Figure 4.3(f) and Table 4.7 show that there is a clear increase in permanent deformation and decrease in stress retention when the number of cycles and the amount of reprocessed content is increased. This trend is consistent for each target elongation. These results indicate a loss in elasticity when the amount of reprocessing cycles and reprocessed content are increased, discussed in 4.1.4.

Figure 4.3(a), Figure 4.3(d), Table 4.7, and Table 4.10 display the comparison between the lab films and the commercial reference films. The permanent deformation of the reference films is slightly higher, while the stress retention lays in the same range for the lab and reference films. This results in a slightly better performance of the lab films, indicating an adequate performance, as established before in the tensile test.

Figure 4.3(b), Figure 4.3(c), Table 4.8, and Table 4.9 present that there is a clear increase in stress retention when temperature is increased. When the temperature is increased to 38°C the permanent deformation increases slightly from 23°C to 38°C for 300% elongation. If the temperature is increased to 60°C the permanent deformation decreases for every target elongation. In summary, when temperature is increased, the stress retention increases and the permanent deformation decreases. As a result, the film gains elasticity when the test temperature is higher.

Slow rate penetration test

The slow rate penetration test was performed to assess the films' resistance to slow punctures. The stretch films may encounter sharp objects or edges during handling and transport, though real-world scenarios would require testing in pre-stretched conditions. The penetration resistance is a critical performance parameter, as it directly relates to their ability to maintain package integrity and protect wrapped goods from damage. The results of the slow rate penetration test are visible in Figure 4.4.

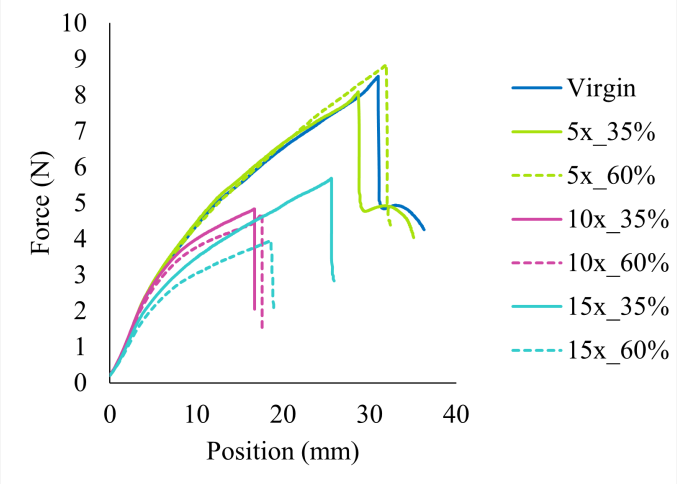

Figure 4.4: Results slow rate penetration test lab films

The **ultimate force** (F_{ultim}) is comparable for the virgin, 5x35%, and 5x60% films. The ultimate force is equal to 8.48 ± 0.516 N, 8.44 ± 0.535 N, and 8.85 ± 0.286 N respectively. The films with 10x35% (4.83 ± 0.247 N), 10x60% (4.70 ± 0.0875 N), 15x35% (5.70 ± 0.186 N), and 15x60% (4.10 ± 0.298 N) reprocessed content show a significant decrease in ultimate force even when the standard deviation is taken into account.

The **ultimate displacement** (D_{ultim}) of the films shows similar results. The virgin film and the two films with 5 times reprocessed content show the highest ultimate displacement at 30.8 ± 1.53 mm, 29.6 ± 1.28 mm, and 32.3 ± 0.963 mm respectively. The films with 10x35% (16.9 ± 0.863 mm), 10x60% (17.3 ± 0.245 mm) and 15x60% (18.0 ± 1.74 mm) times reprocessed content show significantly lower ultimate displacements except for the 15x35% (27.1 ± 1.71 mm) film. Nevertheless, when looking at Figure 4.4 there is a clear difference in the **break energy** (BE) between the 10x35% (0.0546 ± 0.00508 J), 10x60% (0.0543 ± 0.00150 J), 15x35% (0.107 ± 0.0108 J), and 15x60% (0.500 ± 0.00212 J) films and the virgin (0.185 ± 0.0270 J), 5x35% (0.169 ± 0.0210 J), and 5x60% (0.192 ± 0.0126 J) films. The deviation of the 15x35% film can be explained by the fact that the films are made in a pilot scale, possibly leading to diverging manufacturing process settings, resulting in property differences. However, there is still a clear decreasing trend, indicating that films with 5 times reprocessed content maintain mechanical performance in slow rate penetration testing. However, higher reprocessing cycles (10x and 15x) cause significant degradation, further discussed in 4.1.4.

Tear resistance

The tear resistance test was performed to evaluate the films' ability to resist crack propagation once an initial defect of notch is present. This property is crucial for stretch film performance, as it determines whether small defects will lead to catastrophic failure during handling, wrapping, or transport. The tear resistance test lead to the results demonstrated in Figure 4.5 and Figure 4.6, for the lab and commercial reference film respectively.

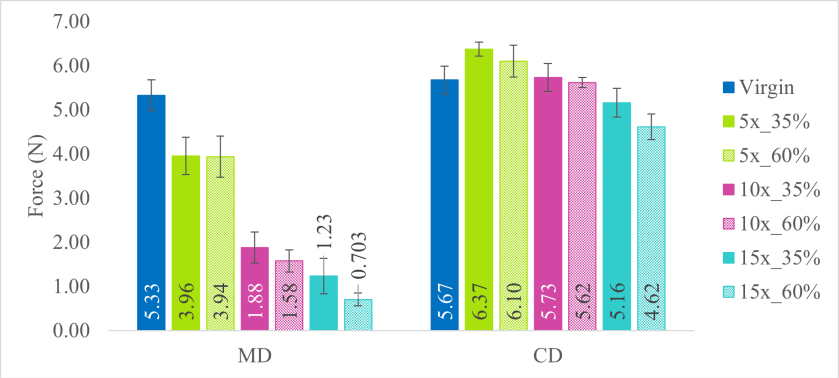

Figure 4.5: Results tear resistance test lab films

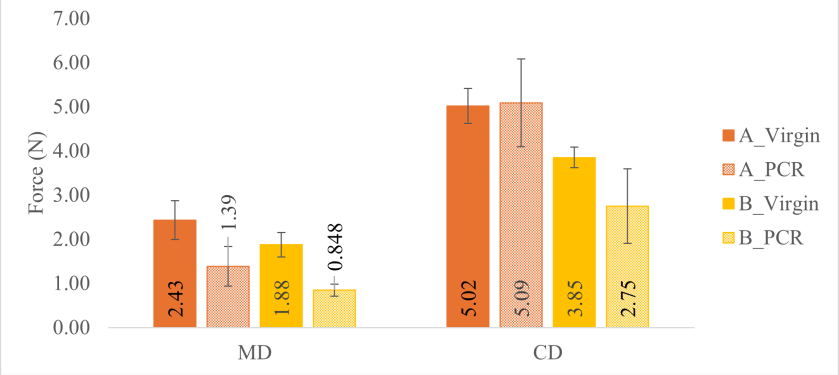

Figure 4.6: Results tear resistance test commercial reference films

Results in Figure 4.5 show a clear decline in MD tear resistance as both reprocessing cycles increase and reprocessed content increases. Even though the thickness of the films decreases with reprocessing, there is a significant decline in tear resistance when going from virgin all the way to the film with 15 times reprocessed content. However, in CD, the tear resistance is much more stable. When taking the standard deviation into account many of the tear resistances overlap when going from the virgin to 15x60% film, especially when the difference in thickness of the films is considered. The commercial reference films also show a clearly lower tear resistance in MD than in CD, with PCR films having a lower tear resistance in MD than the virgin films. In general, most of the lab films show a better tear resistance than the reference films, making their tear resistant performance adequate.

Dart impact test

Dart impact testing was conducted to assess the films' resistance to sudden, high-energy impact that simulates dropping or striking with packed objects. The impact resistance is particularly important for stretch films, which are often used in applications where sudden mechanical shocks may occur during transport or storage. Figure 4.7 visually shows the difference in impact failure weight (W_f). The impact failure weight (W_f) is the weight of the dart at which 50% of the specimens fail during the test. It is a measure to assess the impact resistance of the films. When a film has a high W_f, their resistance to dart impact is better.

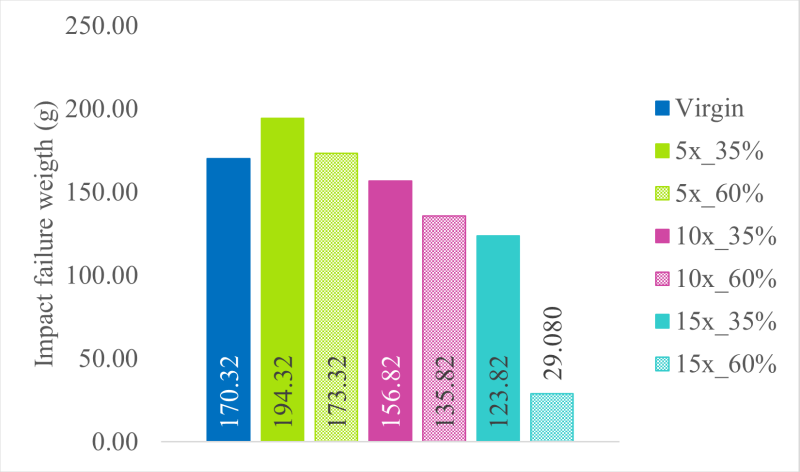

Figure 4.7: Results dart impact test lab films

In the comparison of these results it is important to note that the decrease in thickness with reprocessing plays a role in dart impact performance. The impact failure weight of the 5 times reprocessed films with 35% and 60% reprocessed content is equal to 194.32 g and 173.32 g respectively. These films with 5 times reprocessed content outperform the virgin film, which has an impact failure weight of 170.32 g. The films with 35% and 60% of 10 times reprocessed content show a clear decline to 156.82 g and 135.82 g. The W_f drops even further for the 15 times reprocessed content films. The film with 15x35% reprocessed content shows a small decline to 123.82. Whereas, the 15x60% shows a very low impact failure weight smaller than 29.080 g (lower test limit). This decreasing trend points to the fact that a higher amount of reprocessed content and a higher number of reprocessing cycles, weakens the films' resistance to dart impact. This can be an indicator of a loss of polymer chain integrity and an increased brittleness, explained in 4.1.4.

4.1.3 Transport simulation tests

Tilt test

The 26° angle tilt test was performed to evaluate the films' slip resistance and load retention capabilities under inclined conditions. This test simulates real-world scenarios where wrapped pallets may be stored or transported on sloped surfaces. The tilt test result of each film type is demonstrated in Figure 4.8. All film types passed the tilt test and no significant deformation of the pallets was visible.

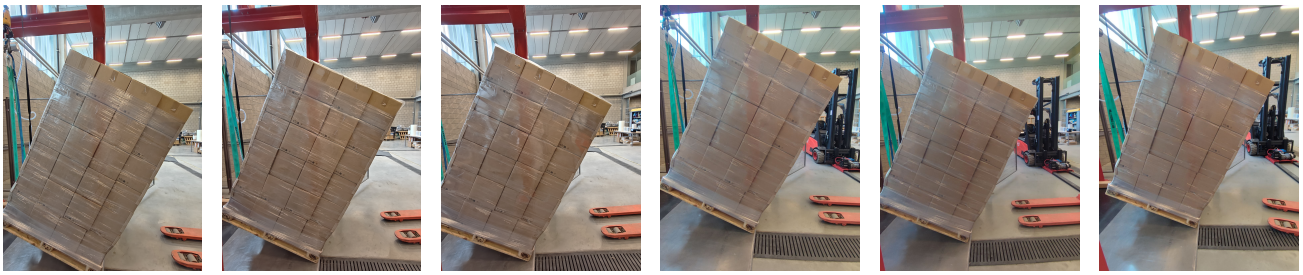

(a) Virgin (b) 5x35% (c) 5x60% (d) 10x35% (e) 10x60% (f) 15x35%

Figure 4.8: Results tilt test lab films

Swing test

The swing test was conducted following the ISTA 3E protocol to evaluate the films' performance under dynamic oscillating loads that simulate the swaying and shifting forces encountered during transportation. Figure 4.9 shows the tilting of the top layers. Figure 4.10 shows the result of the horizontal displacement after the swing test for the top layer and bottom layer.

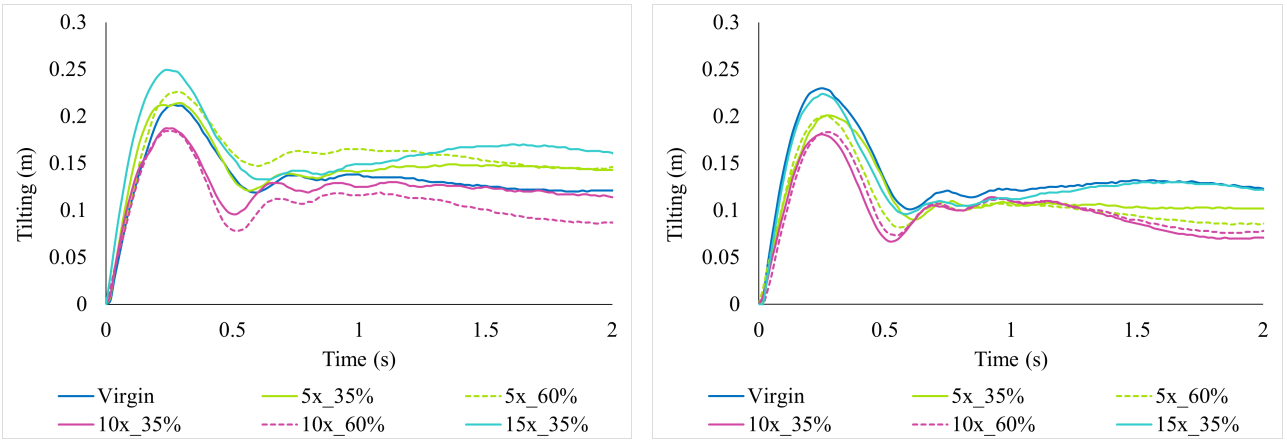

(a) Normal swing test (b) Vibrational pretreatment swing test

Figure 4.9: Results swing test lab films: tilting of top layers

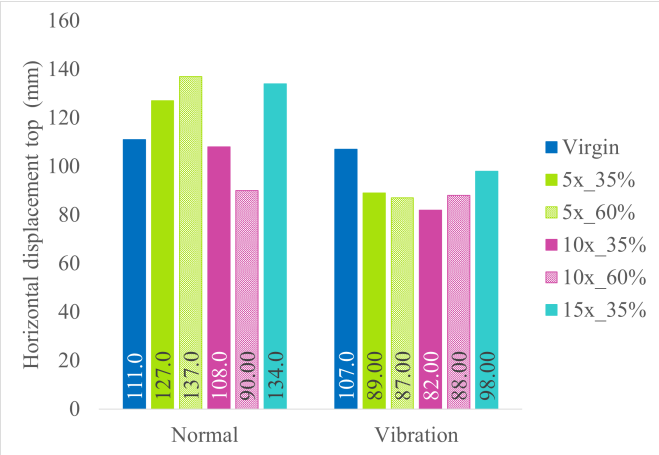

(a) Horizontal displacement top layer

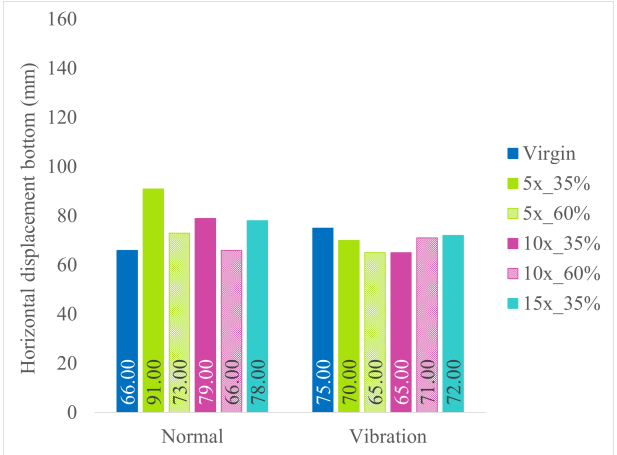

(b) Horizontal displacement bottom layer

Figure 4.10: Results swing test lab film: horizontal displacement top and bottom layer

The results of the tilting during the swing test, displayed in Figure 4.9, show no clear differences across the different films. Additionally, there is no clear difference between the tests performed immediately after wrapping and the tests performed after vibration pretreatment. The films with 10 times reprocessed material seem to have the least amount of tilting while the 15x35% film seems to have the most extensive tilting. Furthermore, no clear trend can be observed when looking at the horizontal displacements of the top and bottom layer, apart from the fact that the top layers show a higher horizontal displacement than the bottom layers. However, the differences in all these results are very minimal and the tests were only performed once so possible test variations are not taken into account. The minimal differences in performance can be a result of the low pre-stretch used in the wrapping process. The small differences that are visible can be a result of the difference in film thickness. The same test was performed on the commercial reference films with and without PCR. The results of these tests show a tilting between 0.15 and 0.20 m for the different films. This is similar to the results of the laboratory films, however comparing both is difficult because the commercial reference films were tested at 150% and 200% pre-stretch. The only film that could not be compared in this test is the worst-case film with 15x60% reprocessed content due to breakage during the wrapping process. The breakage was induced by gauge bands on the film which tore more easily for the films with more reprocessed content and reprocessing cycles, also discussed in 4.1.4.

4.1.4 Material characterisation: discussion

The COF remains more or less the same with increased reprocessing cycles. However, their static and dynamic COF is slightly lower than those of the commercial reference films, potentially because of different outer layer consistencies. A possible hypothesis is that the slightly higher elasticity in the commercial reference films causes an increase in contact surface which increases the friction of the surface. However, the equipment needed to confirm this hypothesis is not available. The lower COF could result in a difference in winding behaviour, cling performance, and load stability. Nevertheless, these differences are very minimal and their consequences on these properties will probably be negligible.

Different polymer degradation mechanisms occur during reprocessing of the material. The most important mechanisms that enter into competition are chain scission and cross-linking. In linear polymers, chain scission typically dominates as the primary degradation pathway. This mechanism reduces polymer molecular weight and fundamentally alters the material's mechanical behaviour by disrupting the entanglement network structure. When polymer chains are shortened, fewer physical entanglements are present between chains, compromising the network that provides mechanical integrity to the material [66, 67]. The weakened entanglement network manifests as reduced stress resistance, since shortened polymer chains can be separated more easily. Ductility is also diminished as the material loses its capacity for extensive deformation before failure, as a result of compromised intermolecular interaction that normally facilitate chain sliding and realignment during plastic deformation. Oxidation products accumulated through repeated reprocessing cycles further contribute to molecular network deterioration by introducing structural defects [66].

DSC results show a slight increase in crystallisation temperature with increased reprocessing which could point to a higher crystallinity in the films with increased reprocessed content. Higher crystallinity may be a result of chain scission, as shorter polymer chains can orient and crystallise more easily than longer chains. However, the results of this test are limited in their statistical reliability, as mentioned before.

GPC and GC-MS tests performed on 1, 5, 10, and 15 times reprocessed granulate, showed results that support the chain scission hypothesis. The decrease in M_n points to more smaller chains as a result of chain scission. The dispersity increases as a result of the larger number of smaller chains in combination with a fewer number of large chains, making the MWD increase. The decrease in primary antioxidant depletion with increased reprocessing, results in a lower amount of antioxidant. The antioxidants can prevent chain scission so their decrease in depletion can induce chain scission.

These chain scission effects are also consistent with the experimental tensile test results, where both stress and strain at break decreased with increasing reprocessed content and reprocessing cycles. The slow rate penetration tests further confirms this mechanism, with a decrease in ultimate force and ultimate displacement. The stress retention test shows increased permanent deformation and decreased stress retention with more reprocessing, pointing to a loss in elasticity and a lower ductility because of chain scission. However, an increase in temperature during this test causes an increase in stress retention and a decrease in permanent deformation, resulting in an increase in elasticity. This is most likely due to increased chain mobility at higher temperatures, resulting in a material that can be stretched with a better stress retention and a better resistance to deformation [68].

The loss in strength is even more clearly pronounced when looking at the tear resistance in MD. The fewer number of entanglements and the shorter chains make that the tear can propagate more easily in-between the polymer chains, because the network between the polymer chains is weaker. However, the tear resistance in CD decreases less severe because the shorter chains cause a more random orientation to tear through in CD. A more detailed explanation is that a Keller-Machin row nucleated structure is formed during quenching. In this structure the crystalline lamellae extend radially from the MD extended chains. Tie molecules that are present in the matrix will connect the crystalline lamellae with covalent bonds. LDPE has a low number of tie molecules due to the large amount of LCB which makes tearing in CD easier. On the contrary, HDPE

and LLDPE have a large number of tie molecules that complicate tears in CD and propagate tears in MD because the van der Waals forces are weaker and easier to break than the covalent bonds [69, 70, 71]. A schematic picture is visible in Figure 4.11. The tin blue lines present the crystalline lamellae, the thick blue lines present the tie molecules, and the red dashed lines represent the break path [69].

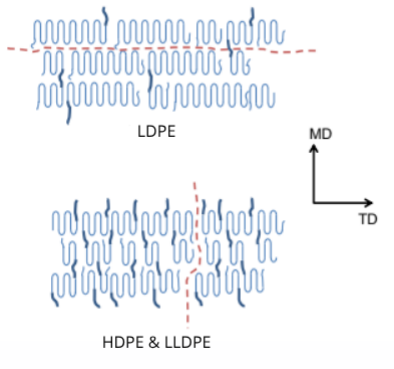

Figure 4.11: Differences in crystalline structure of different PE types [69]

The dart impact test shows similar results, also pointing to chain scission as the primary degradation mechanism. However, in this test a large part of the surface is tested so the film defects could not be avoided. As mentioned before all film rolls have gauge band defects in MD. When reprocessing is increased, these defects have an increased impact on the film's performance, especially in the tests in which these defects could not be avoided such as the dart impact test and also in the wrapping procedure. The increased impact is possibly due to the decrease in MD tear resistance in combination with a reduction in thickness of the films, which causes tears to propagate more easily especially when a defect is already present. The films also show a loss in strength and ductility which attributes to the more pronounced effects of the gauge band defects. This phenomena also manifested itself during the wrapping procedure. The films with 15 times reprocessed content showed rips, visible in Figure 4.12, in the film at the place of the gauge bands when they were wrapped at 100% pre-stretch. The film with 15x35% reprocessed material maintained enough strength to still be wrapped with rips but the film with 15x60% reprocessed material failed every time. The low pre-stretch that is used can be the cause of the small amount of differences in the transport performance tests. An important factor that has to be taken into account is that a lower pre-stretch results in an increased amount of material consumption.

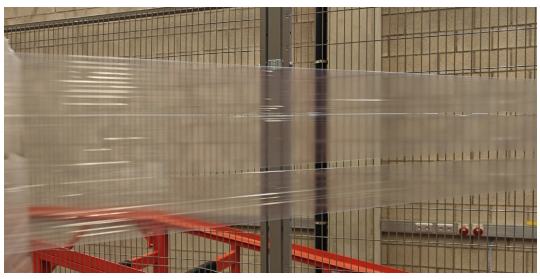

Figure 4.12: Failure during wrapping

4.2 Evaluation of the UV-impact

The impact of UV-exposure on both chemical an mechanical properties was evaluated through accelerated weathering tests conducted over varying exposure periods. One week of exposure is equal to 134.4 h of UVA-light exposure. Most film samples were tested after 5, 8, and 10 weeks of UV-exposure, though the virgin film showed severe degradation and required more frequent testing at weekly intervals for the first 5 weeks. Due to time constraints, the films containing 60% reprocessed content with 10 and 15 reprocessing cycles were evaluated after 3 and 5 weeks of exposure.

4.2.1 Impact on chemical properties

FTIR

FTIR was utilised to identify chemical changes in the polymer structure following UV-exposure, detecting the formation of oxidation products and degradation by-products at the molecular level on both sides of the film. Results of this measurement are shown in Figure 4.13.

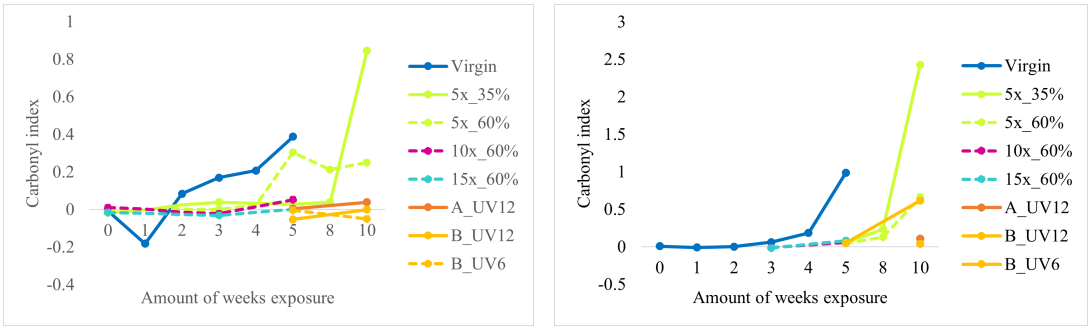

(a) UV-exposed side

(b) Non-exposed side

Figure 4.13: Results FTIR analysis

The results of the FTIR analysis show an increase in CI on both sides of the virgin and 5 times reprocessed films with increased exposure time, pointing to oxidation products formed in the films. The films with 10 and 15 times reprocessed content as well as the commercial reference films with UV-resistant properties have a CI that remains more or less the same on both sides of the film throughout the exposure time. Surprisingly, the CI shows a more pronounced increase on the non-exposed sides of the film. The non-exposed side is the inside of the film, which contains ULLDPE. The outside of the films, the side exposed to UV, consists of only virgin LLDPE. This difference in consistency possibly affects the degradation that takes place. The effect of the consistency on the degradation is discussed in 4.2.3. It should be noted that the FTIR measurements were also performed only once, limiting their statistical reliability.

DSC

DSC was employed to investigate the thermal property changes induced by UV-exposure. It provides insight into how UV-induced degradation affects the polymer's crystalline structure and thermal transitions. The same measurement was performed for the commercial reference films with UV-resistant properties. The DSC curves that were obtained are visible in Figure 4.14.

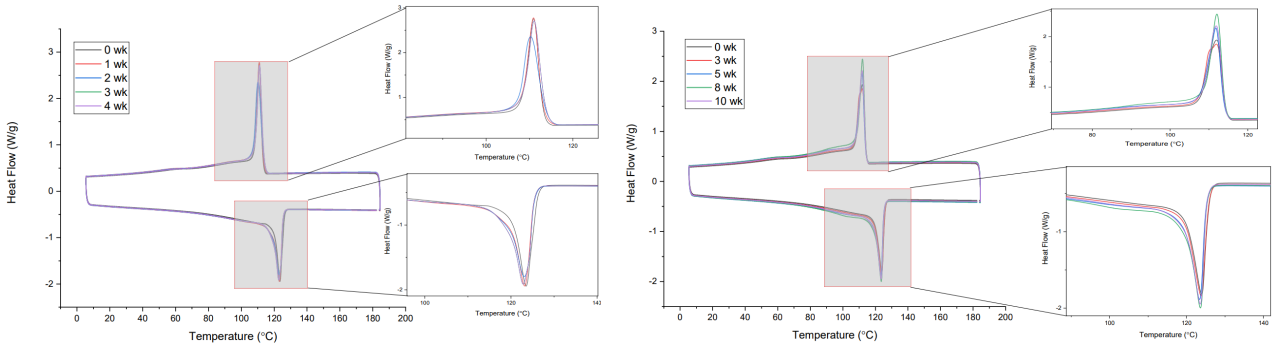

(a) Virgin

(b) 5x35%

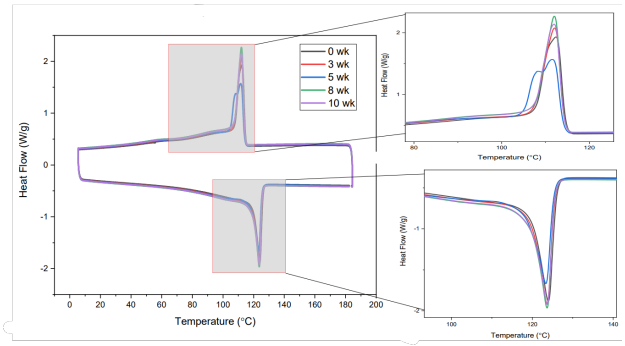

(c) 5x60%

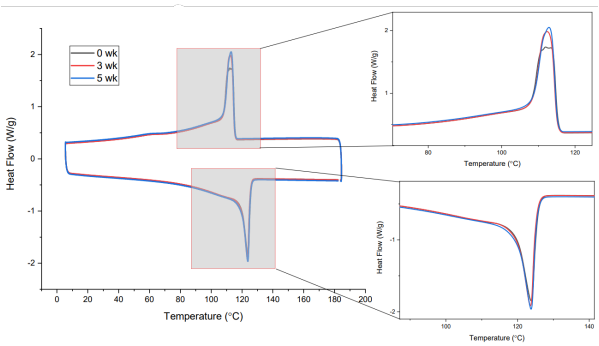

(d) 10x60%

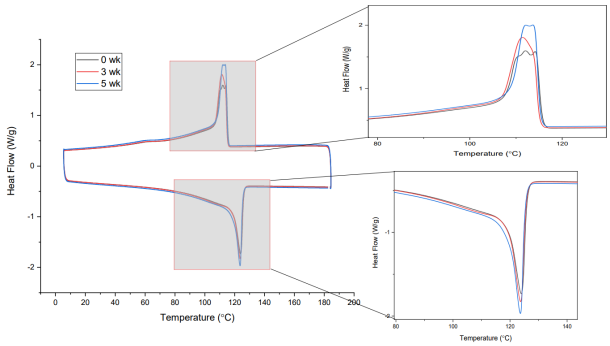

(e) 15x60%

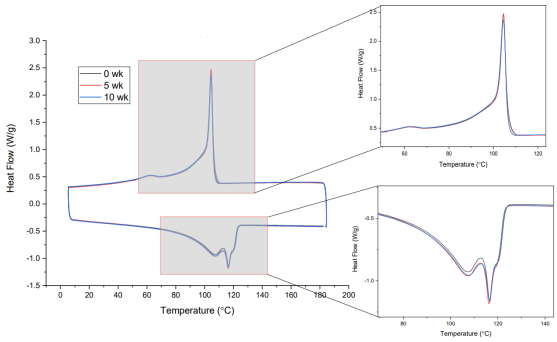

(f) Brand A: 12 months resistance

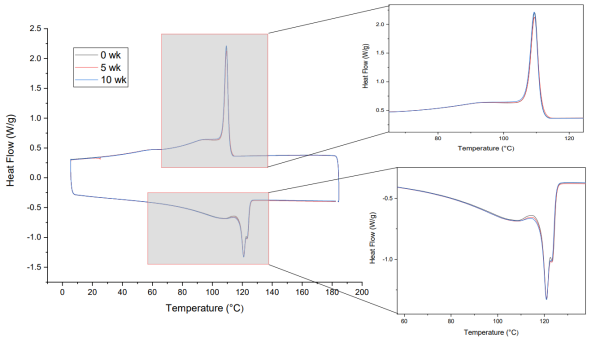

(g) Brand B: 6 months resistance

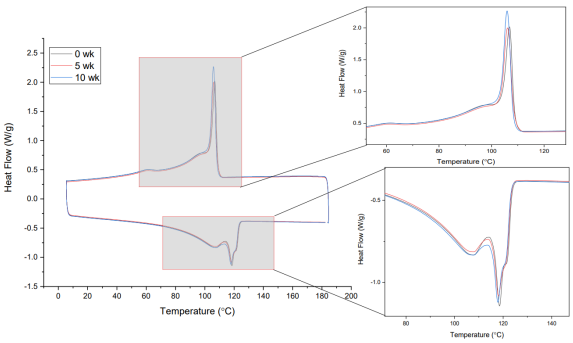

(h) Brand B: 12 months resistance

Figure 4.14: Results DSC after UV-exposure

There are no clear trends or differences detected for the crystallisation and melting temperature as well as the degree of crystallinity. The last three curves show the results of the commercial reference films with UV-resistant properties. The crystallisation and melting temperature of these films remains constant throughout UV-exposure, pointing to limited degradation.

4.2.2 Impact on mechanical properties

Tensile test

UV-exposure can induce degradation which possibly influences the film's mechanical performance. This tensile test gives an indication of mechanical performance of the films after UV-exposure. Figure 4.15 displays the results of the tensile test after UV-exposure for the different films.

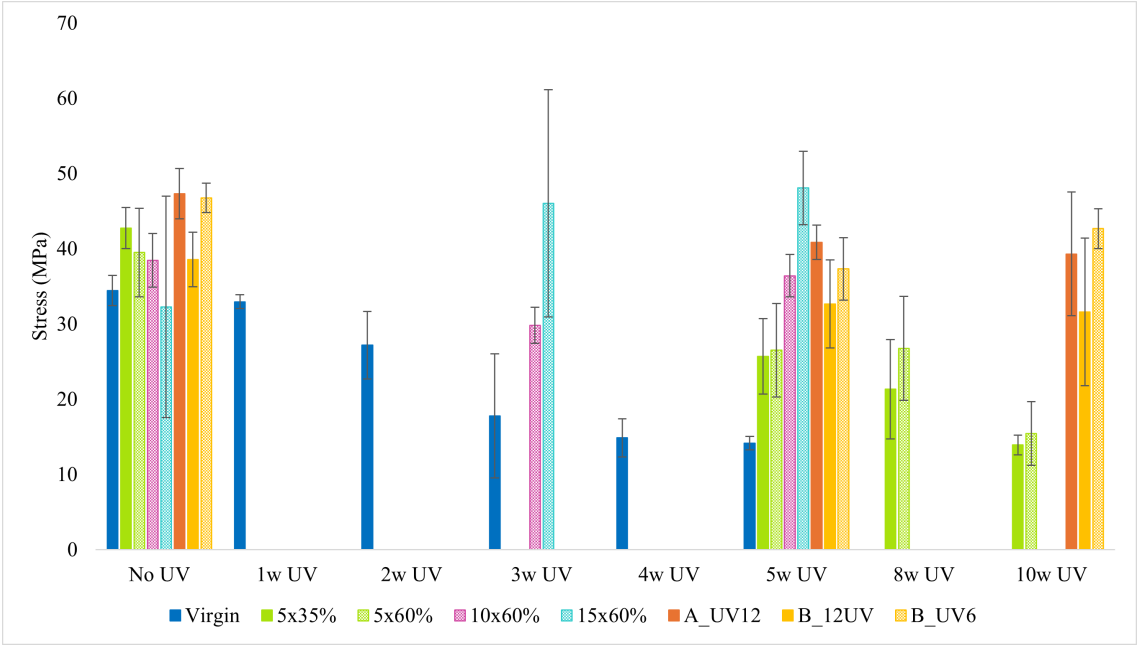

(a) Stress at break after UV

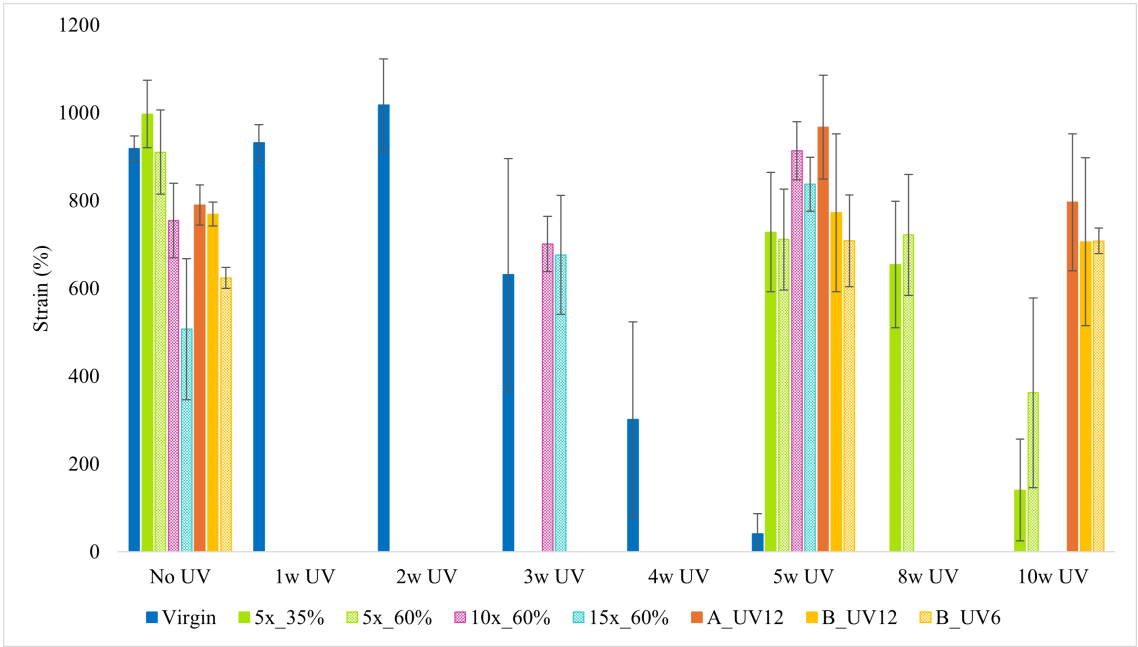

(b) Strain at break after UV

Figure 4.15: Results tensile test after UV-exposure

These results show that for the virgin and 5 times reprocessed films the stress and strain at break decrease with increased UV-exposure, with virgin film showing the most significant decrease. The stress and strain at break remain constant for the film with 10x60% reprocessed content as well

as the commercial reference films with UV-resistant properties. However, the film with 15x60% reprocessed content shows an increase in stress and strain at break. This is a remarkable result, as the films with reprocessed content do not seem to have a high sensitivity to UV-light exposure.

Stress-relaxation test at 200%

The stress-relaxation test performed on the films that were treated with the UV-cycle in the QUV-machine lead to the results in Figure 4.16. These results show the impact of UV-light on the hysteresis loop of these stretch films and give an indication of the impact on the films' elasticity.

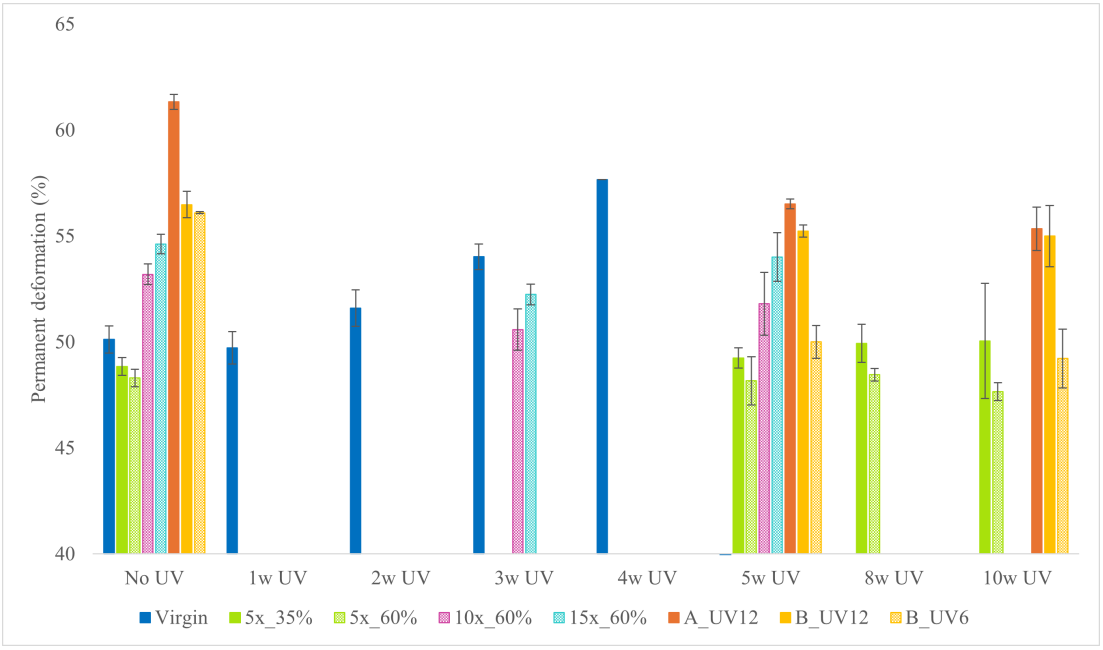

(a) Permanent deformation after UV

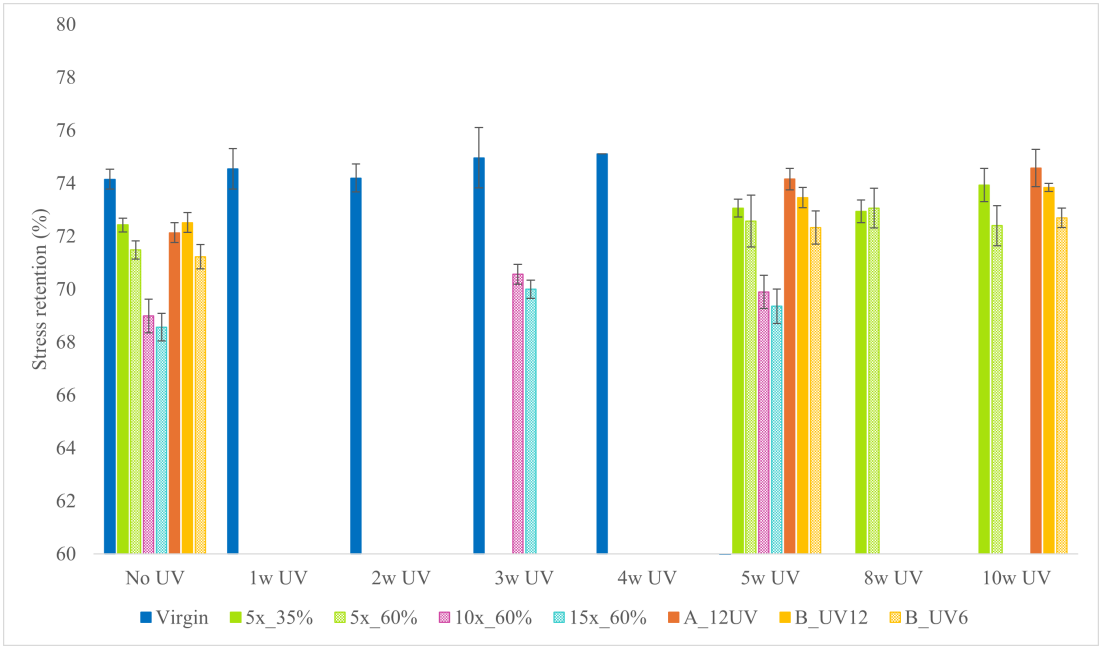

(b) Stress retention after UV

Figure 4.16: Results stress-relaxation test after UV-exposure

There were no significantly different results attained during this test. Stress retention remains stable for all films exposed to UV, implying that the stress retention is not influenced by UV-exposure. Permanent deformation of the virgin film and the 5x35% film increases slightly with longer exposure times. The permanent deformation of the other films remains stable throughout exposure and is not sensitive to UV-light. In comparison, all commercial reference films, that have UV-resistant properties of 6 and 12 months, show a decrease in permanent deformation and increase in stress retention with increased exposure, indicating increased elasticity.

The most significant difference in this test lays in the number of failed tests. For each film type only five tests were performed per time interval. The number of failed tests out of these five tests was monitored. First, the virgin film failed once after three weeks of exposure, 4 times after four weeks of exposure, and 5 times after five weeks of exposure. Second, the film with 5x35% reprocessed content failed twice after eight weeks of exposure and twice after ten weeks. Third, the film with 5x60% of reprocessed content failed one time after ten weeks of UV-exposure. Last, the films with 10x60% and 15x60% reprocessed content did not fail in the first five weeks of exposure.

4.2.3 Impact of UV on mechanical and chemical properties: discussion

The results of the DSC show no clear trends and are limited in their statistical reliability, as mentioned before. The commercial reference films with UV-resistant properties seem to remain constant, indicating that no degradation takes place.

The results of the FTIR test on the exposed and non-exposed side of the films exhibited that the non-exposed side showed a more significant increase in CI. The inside of the film was not exposed to UV-light and consists of a 50:50 combination of ULLDPE and virgin LLDPE. The UV-exposed side consists only of virgin LLDPE. ULLDPE contains more amorphous regions than LLDPE, due to its lower density. Because oxidation-induced cracks nucleate in the amorphous phase of the polymer, the ULLDPE is more prone to oxidative degradation. The sensitivity to oxidative degradation leads to a possible increase in CI [72, 73, 74].

The tensile test showed that these films show a decrease in stress and strain at break when the exposure time is increased. The decrease in tensile properties seems to point to the same chain scission effect that occurs when reprocessing is increased [66, 67]. This leads to the hypothesis that UV-light exposure leads to chain scission as the primary degradation pathway. The results of the FTIR support this hypothesis as the CI of these films increases with exposure time. An increase in CI means that these films underwent oxidation degradation. This surface oxidation, with formation of carbonyl groups, also points to chain scission as the primary degradation pathway [74]. The number of fails in the stress-retention test provide additional support to this hypothesis. The increase in fails shows that the virgin and 5 times reprocessed films become more brittle and less elastic. A more brittle and less elastic film is also a result of oxidative degradation and chain scission [74].

On the contrary, the films with a higher number of reprocessing cycles seem to have a better resistance to UV-induced degradation. The 10 times reprocessed film shows tensile properties that remain constant with increased exposure time and the 15 times reprocessed film seems to have increased tensile properties. Their CI determined with FTIR remains constant, suggesting no UV-induced oxidation and chain scission take place because no additional carbonyl groups are formed. Furthermore, the stress-retention test could be performed without fails for these films. A possible explanation for this resistance against UV-exposure is that the concentration of HALS is higher in films with more reprocessing cycles. These HALS protect the films against UV-degradation. This hypothesis can be confirmed by further research investigating the HALS concentration in the different films.

The commercial reference films with UV-resistance are additivated with UV-stabilisers that act as radical scavengers in the degradation process, inhibiting chain scission. The two UV-resistant films from brand B also have a white pigment that can further inhibit degradation because the UV-light is reflected by the pigment.

Chapter 5

Conclusion

This research investigated the impact of reprocessed content and multiple reprocessing cycles on the performance of PE stretch films for palletised loads, with particular focus on chemical characteristics, mechanical properties, transport performance, and UV-resistance.

5.1 Chemical characteristics

The chemical characterisation revealed minimal changes in thermal properties with increased reprocessing. The DSC results showed a slight increase in crystallisation temperatures with higher reprocessing cycles, potentially indicating increased crystallinity in films with more reprocessed content and more reprocessing cycles.

GPC and GC-MS analyses provided crucial evidence supporting chain scission as the primary pathway. They demonstrated an increase in dispersity and a decrease in number average molecular weight with increase reprocessing cycles. Primary antioxidant depletion decreased, which further accelerates chain scission by reducing the film's protection against oxidative degradation. Additionally, the depletion of secondary antioxidants probably decreases as well, enhancing chain scission.

5.2 Mechanical properties

Chain scission emerged as the dominant degradation mechanism during reprocessing, leading to systematic deterioration in mechanical properties. Both stress and strain at break decreased with increasing reprocessed content (35% vs 60%) and reprocessing cycles (5, 10, and 15). This degradation was attributed to reduced molecular weight and weakened entanglement networks, resulting in diminished stress resistance and ductility.

The effects were particularly pronounced in MD tear resistance, where fewer entanglements and shorter chains facilitated easier tear propagation. The directional dependency of tear resistance was explained by the Keller-Machin row nucleated structure. Stress-retention tests confirmed increased permanent deformation and reduced elasticity with more reprocessing. Even though, elevated temperatures during testing demonstrated improved chain mobility and stress retention. Dart impact tests further supported the chain scission hypothesis while revealing the significant impact of gauge band defects on film performance as processing increased.

5.3 Transport performance

During wrapping procedures practical limitations became evident. Films with 15 reprocessing cycles and 60% reprocessed content failed consistently due to gauge band defects, while films with 15x35% reprocessed content maintained adequate wrapping capability at a maximum pre-stretch of 100%. The interaction between reduced MD tear resistance, decreased film thickness, and pre-existing gauge band defects created critical failure points during the high-stress wrapping process.

Despite the mechanical property degradation, transport performance tests showed minimal differences between the films that could be tested (all except 15x60% film). This was attributed to the low pre-stretch used during testing. Another relevant consideration is that the thickness of the films plays a role in their performance as well, making possible interpretations more difficult. However, it should be noted that films that are wrapped at lower pre-stretch values have a higher material consumption.

5.4 UV-resistance

UV-exposure revealed contrasting behaviours depending on the initial film composition and reprocessing history. Virgin and lightly (5 times) reprocessed films showed significant degradation under UV-exposure. They showed decreased tensile properties and an increased CI indicating oxidation followed by chain scission as the primary degradation pathway. The greater carbonyl group formation on the non-exposed side, was attributed to consistency of the inner layer that incorporates ULLDPE. ULLDPE has a lower density and more amorphous content, which is more susceptible to oxidative degradation.

Conversely, films with a higher number of reprocessing cycles (10 and 15) and a high amount of reprocessed content (60%) demonstrated improved UV-resistance, with constant or even enhanced properties upon exposure. This unexpected finding suggests that higher concentrations of HALS in these films may provide enhanced protection against UV-induced degradation. The commercial reference films with UV-resistance maintained consistent properties, confirming the effectiveness of UV-stabiliser additives in preventing degradation.

5.5 Overall conclusion

The research demonstrates that while mechanical reprocessing inevitably degrades film properties through primarily chain scission, stretch films can accommodate moderate levels of reprocessed content while maintaining acceptable performance for transport applications.

Critical performance thresholds exist beyond which films become unsuitable for demanding applications. Particularly at high reprocessed content levels (60%) combined with extensive reprocessing cycles (15). The interaction between mechanical degradation and pre-existing defects, such as gauge bands, creates failure points that have to be accounted for.

The trade-off between sustainability through recycled material incorporation and performance degradation must be carefully balanced. In this balance factors such as material consumption, pre-stretch requirements, end-use applications, and the distinction between reprocessed content and PCR content must be considered.

This study indicates that the PPWR goal of 35% recycled content by 2030 is achievable. However, the incorporation of 65% recycled content in stretch films remains a challenge, because of severe decreases in performance due to degradation. To achieve this goal by 2040, further research on this topic in the upcoming years is crucial.

An important consideration is that no additional antioxidants were added during reprocessing in this study, as the objective was to understand what the consequences were on the film performance. While the results show that functional films can still be produced under these conditions, the observed antioxidant depletion and subsequent chain scission suggest that incorporating fresh antioxidants during reprocessing could be a beneficial practice to mitigate performance degradation.

5.6 Recommendations for future research

Future work should focus on several key areas to strengthen the scientific foundation and practical applicability of this research.

- **Study on the performance of reprocessed films with addition of antioxidant**

  Conducting a study on reprocessed films in which the reprocessed material is additivated with antioxidants. The amount of antioxidant that is added can be matched with the antioxidant depletion that takes places during reprocessing. Additionally, it could also be interesting to see what happens when there is no antioxidant present in the virgin granulate. However, this is not possible for LLDPE but it is possible for LDPE which could also lead to interesting results.

- **Crystalline morphology analysis:**

  Investigating the crystalline structure using techniques such as Scanning Electron Microscopy (SEM), X-Ray diffraction (XRD), Wide Angle X-ray Scattering (WAXS), and Small Angle X-ray Scattering (SAXS). This investigation can support the hypotheses of the relationship between crystalline morphology, and mechanical and transport performance.

- **UV-stabiliser investigation:**

  Further investigation of the HALS concentration and depletion patterns across the different films to validate the hypothesis that explains the improved UV-resistance in highly reprocessed films.

- **Real-world correlation studies:**

  Performing additional analyses to investigate the differences between controlled reprocessing and real-world recycling to establish stronger correlations between laboratory findings and practical applications. Possible pathways include the effects of elevated processing temperatures (e.g., 250°C) that may occur in industrial settings and the influence of contaminants typical in actual recycling streams.

Acknowledgement

I acknowledge the use of claude.ai (https://claude.ai/) to refine academic language and writing [75]. The output was critically modified with care and attention to accuracy of the content.

References

[1] UHasselt, "MultiRec," 2022. [Online]. Available: https://www.uhasselt.be/nl/onderzoeksgroepen/imo-imomec-materials-and-packaging-research-services/onderzoek/multirec-2022. [Accessed: Feb. 21, 2025].

[2] European Commission, "Packaging waste," 2025. [Online]. Available: https://environment.ec.europa.eu/topics/waste-and-recycling/packaging-waste. [Accessed: Mar. 4, 2025].

[3] EUROPEN, "Packaging and Packaging Waste Regulation," 2025. [Online]. Available: https://www.europen-packaging.eu/policy-area/packaging-and-packaging-waste-directive/. [Accessed: Mar. 4, 2025].

[4] K. L. Yam, *The Wiley Encyclopedia of Packaging Technology*. 3 ed., 2010. Available: https://books.google.be/books/about/The_Wiley_Encyclopedia_of_Packaging_Tech.html?id=LW1lxnnMi94C&redir_esc=y.

[5] B. A. Morris, "Commonly used resins and substrates in flexible packaging," *The Science and Technology of Flexible Packaging*, pp. 69–119, Jan. 2017. doi: 10.1016/B978-0-323-24273-8.00004-6.

[6] ISO 527-3:2018, "Plastics — Determination of tensile properties — Part 3: Test conditions for films and sheets," 2018. Available: https://www.iso.org/standard/70307.html.

[7] ASTM D882-02, "Test Method for Tensile Properties of Thin Plastic Sheeting," 2002. Available: https://www.astm.org/d0882-02.html.

[8] ASTM F1306 2016, "Standard Test Method for Slow Rate Penetration Resistance of Flexible Barrier Films and Laminates 1," 2016. Available: https://doi.org/10.1520/F1306-16.

[9] ASTM D5748, "Test Method for Protrusion Puncture Resistance of Stretch Wrap Film," 2019. Available: https://doi.org/10.1520/D5748-95R19.

[10] ASTM D1709 2003, "Standard Test Method for Impact Resistance of Plastic Film by the Free-Falling Dart Method," 2003. doi: 10.1520/D1709-24.

[11] EN ISO 8295:2004, "Plastics - Film and sheeting - Determination of the coefficients of friction," 2004. Available: https://standards.iteh.ai/catalog/standards/cen/ea903b24-990f-4761-8c14-f9c0b0d0f50d/en-iso-8295-2004?srsltid=AfmBOorTme7Cm9GxCIbNXo9QsXrOxtTdPJ0l0J4M4-mfl9wiNxIvqvtQ.

[12] ASTM D1894, "Test Method for Static and Kinetic Coefficients of Friction of Plastic Film and Sheeting," 2014. Available: https://doi.org/10.1520/D1894-14.

[13] EN ISO 6383-2:2004, "Plastics - Film and sheeting - Determination of tear resistance - Part 2: Elmendorf method," 2004. Available: https://standards.iteh.ai/catalog/standards/cen/7af81cca-1a63-4fae-a297-61bb94cf5dab/en-iso-6383-2-2004?srsltid=AfmBOoogIAgoT4ZEuLuRNQSoaEHEirS761HUttzP_G-Xin-myv4igIaB.

[14] ASTM D5459, "Test Method for Machine Direction Elastic Recovery and Permanent Deformation and Stress Retention of Stretch Wrap Film," 2020. Available: https://doi.org/10.1520/D5459-95R20.

[15] ISTA, "Overview of Procdure 3E," 2017.

[16] ISO 4892-1:2016, "Plastics — Methods of exposure to laboratory light sources — Part 1: General guidance," 2016. Available: https://www.iso.org/standard/60048.html.

[17] ISO 4892-3:2016, "Plastics — Methods of exposure to laboratory light sources — Part 3: Fluorescent UV lamps," 2016. Available: https://www.iso.org/standard/67793.html.

[18] Z. O. G. Schyns, M. P. Shaver, Z. O. G. Schyns, and M. P. Shaver, "Mechanical recycling of packaging plastics: A review," *Macromolecular Rapid Communications*, vol. 42, p. 2000415, Feb. 2021. doi: 10.1002/MARC.202000415.

[19] Ellen MacArthur Foundation, "What is a circular economy?." [Online] Available: https://www.ellenmacarthurfoundation.org/topics/circular-economy-introduction/overview [Accessed: Apr. 07, 2025].

[20] Statbel, "Packaging waste," 2024. [Online]. Available: https://statbel.fgov.be/nl/themas/leefmilieu/afval-en-vervuiling/verpakkingsafval#news [Accessed: Apr. 10, 2025].

[21] EU monitor, "Directive 1994/62 - Packaging and packaging waste." [Online] Available: https://www.eumonitor.eu/9353000/1/j4nvk6yhcbpeywk_j9vvik7m1c3gyxp/vitgbghutpzz [Accessed: Apr. 07, 2025].

[22] Sinyar Packagin Film, "Basic knowledge of stretch film." [Online] Available: https://www.plasticwraproll.com/basic-knowledge-of-stretch-film/ [Accessed: Apr. 07, 2025].

[23] L. K. Rogers, "Equipment 101: Unitizing equipment," *Modern Materials Handling*, Jul. 2011. Available: https://www.mmh.com/article/equipment_101_unitizing_equipment.

[24] Laundrie, "Unitizing goods on pallets and slipsheets general technical report," 1986.

[25] Matco International, "Opening Experience Center!." [Online]Available: https://matco-international.com/nl/opening-experience-center/ [Accessed: Apr. 07, 2025].

[26] L. P. with innovation, "Is paper pallet wrap the future?," Dec. 2023. Available: https://www.lindumpackaging.com/resources/is-paper-pallet-wrap-the-future/.

[27] R. Coles, D. McDowell, and M. J. Kirwan, "Food packaging technology," pp. 189–191, 2003. Available: www.blackwellpublishing.com.

[28] P. C. Dartora, R. M. C. Santana, and A. C. F. Moreira, "The influence of long chain branches of lldpe on processability and physical properties," *Polimeros*, vol. 25, pp. 531–539, Nov. 2015. doi: 10.1590/0104-1428.1732.

[29] B. M. Weckhuysen and R. A. Schoonheydt, "Olefin polymerization over supported chromium oxide catalysts," *Catalysis Today*, vol. 51, pp. 215–221, Jun. 1999. doi: 10.1016/S0920-5861(99)00046-2.

[30] L. Poh, Q. Wu, Y. Chen, and E. Narimissa, "Characterization of industrial low-density polyethylene: a thermal, dynamic mechanical, and rheological investigation," *Rheologica Acta*, vol. 61, pp. 701–720, Oct. 2022. doi: 10.1007/S00397-022-01360-1/TABLES/6.

[31] F. Sadeghi and A. Ajji, "Application of single site catalyst metallocene polyethylenes in extruded films: Effect of molecular structure on sealability, flexural cracking and mechanical properties," *The Canadian Journal of Chemical Engineering*, vol. 92, pp. 1181–1188, Jul. 2014. doi: 10.1002/CJCE.21964.

[32] R. W. Halle and A. M. Malakoff, "A new high-performance mvldpe," *Journal of Plastic Film and Sheeting*, vol. 21, pp. 13–26, Jan. 2005. doi: 10.1177/8756087905050671.

[33] H. Münstedt, "Extensional rheology and processing of polymeric materials," *International Polymer Processing*, vol. 33, pp. 594–618, 2018. doi: 10.3139/217.3532.

[34] V. Marturano, P. Cerruti, and V. Ambrogi, "Polymer additives," *Physical Sciences Reviews*, vol. 2, Jun. 2019. doi: 10.1515/PSR-2016-0130/ASSET/GRAPHIC.

[35] V. Ambrogi, C. Carfagna, P. Cerruti, and V. Marturano, "Additives in polymers," *Modification of Polymer Properties*, pp. 87–108, Jan. 2017. doi: 10.1016/B978-0-323-44353-1.00004-X.

[36] B. SE, "Irgafos 168 - costabilizer antioxidant," Sep. 2017.

[37] B. SE, "Irganox 1076," Feb. 2019.

[38] J. Christmann, J. L. Gardette, G. Pichon, B. Bouchut, and S. Therias, "Photostabilization of polyethylene by a hindered amine light stabilizer in blooming conditions and impact of mdo processing," *Polymer Degradation and Stability*, vol. 191, p. 109683, Sep. 2021. doi: 10.1016/J.POLYMDEGRADSTAB.2021.109683.

[39] R. K. III and S. S. Woods, "The influence of polymer process aid (ppa) and hindered amine light stabilizer (hals) combinations in lldpe blown film applications: Part 2b," Jan. 2000.

[40] CIBA, "Chimassorb 944," May 2002.

[41] H. Zhou, X. Hu, M. Liu, and D. Yin, "Benzotriazole ultraviolet stabilizers in the environment: A review of analytical methods, occurrence, and human health impacts," *TrAC Trends in Analytical Chemistry*, vol. 166, p. 117170, Sep. 2023. doi: 10.1016/J.TRAC.2023.117170.

[42] M. Rennert, S. Fiedler, M. Nase, M. Menzel, S. Günther, J. Kressler, and W. Grellmann, "Investigation of the migration behavior of polyisobutylene with various molecular weights in ethylene/-olefin copolymer blown stretch films for improved cling properties," *Journal of Applied Polymer Science*, vol. 131, p. 40239, May 2014. doi: 10.1002/APP.40239.

[43] G. M. Mcnally, C. M. Small, W. R. Murphy, A. H. Clarke, and G. M. McNally, "The effect of pib molecular weight on the cling characteristics of polyethylene-pib films for stretch and cling film applications," *Applications. Journal of Plastic Film and Sheeting*, vol. 21, 2005. doi: 10.1177/8756087905052805ï.

[44] J. Pionteck and G. Wypych, *Handbook of Antistatics*. ChemTec Publishing, Jan. 2007. Available: https://books.google.be/books?id=FENOSQoBHw4C&printsec=copyright&redir_esc=y#v=onepage&q&f=false.

[45] S. Zhao, M. Zheng, and K. Shen, "Ultrasound-assisted preparation of highly dispersion sulfonated graphene and its antistatic properties," *The Journal of The Textile Institute*, vol. 112, pp. 30–36, 2021. doi: 10.1080/00405000.2020.1746010.

[46] J. Wu, W. Wang, X. Chen, and N. Li, "Double percolation and segregated structures formed in polymer alloy with excellent electrical conductivity," *Polymer Composites*, vol. 42, pp. 693–700, Feb. 2021. doi: 10.1002/PC.25858.

[47] G. Yakovlev, G. Pervushin, O. Smirnova, E. Begunova, and Z. Saidova, "The electrical conductivity of fluoroanhydrite compositions modified at the nanoscale level with carbon black," *Environmental and Climate Technologies*, vol. 24, pp. 706–717, Jan. 2020. doi: 10.2478/RTUECT-2020-0044.

[48] C. Zhang, Y. Cui, S. Lin, and J. Guo, "Preparation and applications of hydrophilic quaternary ammonium salt type polymeric antistatic agents," *E-Polymers*, vol. 22, pp. 370–378, Jan. 2022. doi: 10.1515/EPOLY-2022-0035.

[49] T. Matyja, "Determining the optimal number of stretch film layers for ensuring palletized cargo stability: A simulation study," *Scientific Journal of Silesian University of Technology*, vol. 124, pp. 93– 108, 2024. doi: 10.20858/sjsutst.2024.124.7.

[50] Álvaro Garrido-López, V. Esquiu, and M. T. Tena, "Comparison of three gas chromatography methods for the determination of slip agents in polyethylene films," *Journal of Chromatography A*, vol. 1150, pp. 178–182, May 2007. doi: 10.1016/J.CHROMA.2006.11.090.

[51] C. Llop, A. Manrique, R. Navarro, C. Mijangos, and H. Reinecke, "Control of the migration behavior of slip agents in polyolefin-based films," *Polymer Engineering Science*, vol. 51, pp. 1763–1769, Sep. 2011. doi: 10.1002/PEN.21963.

[52] A. Riley, "Plastics manufacturing processes for packaging materials," *Packaging Technology*, pp. 310–360, Jan. 2012. doi: 10.1533/9780857095701.2.310.

[53] R. J. Crawford and P. J. Martin, "Processing of plastics," *Plastics Engineering*, pp. 279–409, Jan. 2020. doi: 10.1016/B978-0-08-100709-9.00004-2.

[54] R. F. Nunes, *Wrapping Machinery, Stretch-Film*, pp. 973–978. Wiley, 2 ed., 1997.

[55] T. K. Park and K. H. Kim, "Comparing handling and space costs for various types of stacking methods," *Computers Industrial Engineering*, vol. 58, pp. 501–508, Apr. 2010. doi: 10.1016/J.CIE.2009.11.011.

[56] EasyCargo, "Column stacking vs. interlocking stacking," 2023. [Online]. Available: https://www.easycargo3d.com/en/blog/column-stacking-vs-interlocking-stacking/. [Accessed: Apr. 10, 2025].

[57] Revolution, "5 questions you should be asking about post-consumer recycled (pcr) resin used in flexible films - revolution sustainable solutions," Available: https://www.revolutioncompany.com/blog/5-questions-you-should-be-asking-about-post-consumer-recycled-pcr-resin-used-in-flexible-films/.

[58] Raja, "Home." [Online]. Available: https://www.raja-group.com/ [Accessed: Apr. 10, 2025].

[59] Coeman End-of-line Packaging Specialist, "Home." [Online]. Available: https://www.coeman.be/en [Accessed: Apr. 10, 2025].

[60] Darco, "Pack to Protect: Solutions for stable pallets and safe transport." [Online]. Available: https://www.darco.eu/en [Accessed: Apr. 10, 2025].

[61] G. Cabrera, J. Li, A. Maazouz, and K. Lamnawar, "A journey from processing to recycling of multilayer waste films: A review of main challenges and prospects," *Polymers 2022, Vol. 14, Page 2319*, vol. 14, p. 2319, Jun. 2022. doi: 10.3390/POLYM14122319.

[62] K. Ragaert, L. Delva, and K. V. Geem, "Mechanical and chemical recycling of solid plastic waste," *Waste Management*, vol. 69, pp. 24–58, Nov. 2017. doi: 10.1016/J.WASMAN.2017.07.044.

[63] Drug Plastics Glass Co., Inc., "Mechanical Recycling." [Online]. Available: https://www.drugplastics.com/sustainability/mechanical-recycling [Accessed: Apr. 10, 2025].

[64] E. 40509:2012, "Test method for load unit rigidity," 2020. [Online]. Available: https://eumos.eu/eumos-40509-2020-test-method-for-load-unit-rigidity/ [Accessed: Apr. 10, 2025].

[65] M. Celik, H. Nakano, K. Uchida, A. Isobe, and H. Arakawa, "Comparative evaluation of the carbonyl index of microplastics around the japan coast," *Marine Pollution Bulletin*, vol. 190, p. 114818, May 2023. doi: 10.1016/J.MARPOLBUL.2023.114818.

[66] A. A. Mendes, A. M. Cunha, and C. A. Bernardo, "Study of the degradation mechanisms of polyethylene during reprocessing," *Polymer Degradation and Stability*, vol. 96, pp. 1125–1133, Jun. 2011. doi: 10.1016/J.POLYMDEGRADSTAB.2011.02.015.

[67] A. Felgel-Farnholz, A. Schweighuber, C. W. Klampfl, and J. Fischer, "Comparative study on the degradation of hdpe, lldpe and ldpe during multiple extrusions," *Polymer Degradation and Stability*, vol. 216, p. 110486, Oct. 2023. doi: 10.1016/J.POLYMDEGRADSTAB.2023.110486.

[68] W. Luo, W. Chen, D. Liu, X. Huang, and B. Ma, "Effect of temperature and humidity on mechanical properties and constitutive modeling of pressure-sensitive adhesives," *Scientific Reports*, vol. 14, p. 14634, Dec. 2024. doi: 10.1038/S41598-024-64960-2.

[69] B. A. Morris, "Strength, stiffness, and abuse resistance," *The Science and Technology of Flexible Packaging*, pp. 309–350, Jan. 2017. doi: 10.1016/B978-0-323-24273-8.00009-5.

[70] X. M. Zhang, S. Elkoun, A. Ajji, and M. A. Huneault, "Oriented structure and anisotropy properties of polymer blown films: Hdpe, lldpe and ldpe," *Polymer*, vol. 45, pp. 217–229, Jan. 2004. doi: 10.1016/J.POLYMER.2003.10.057.

[71] L. I. W. Lee, R. A. Register, and D. M. Dean, "Origin of directional tear in blown films of ethylene/methacrylic acid copolymers and ionomers," *Journal of Polymer Science Part B: Polymer Physics*, vol. 43, pp. 97–106, Jan. 2005. doi: 10.1002/POLB.20309.

[72] B. Zhao and M. A. Zikry, "Oxidation-induced failure in semi-crystalline organic thin films," *International Journal of Solids and Structures*, vol. 109, pp. 72–83, 3 2017. doi: 10.1016/J.IJSOLSTR.2017.01.008.

[73] M. C. Özdemir, Ülkü Dide Türkeli, R. Çaliskan, and İpek İmamoglu, "Impact of accelerated uv aging on chemical structure and sorption behavior of low-density polyethylene microplastics," *Journal of Environmental Chemical Engineering*, vol. 13, p. 116645, 6 2025. doi: 10.1016/J.JECE.2025.116645.

[74] E. Syranidou, K. Karkanorachaki, D. Barouta, E. Papadaki, D. Moschovas, A. Avgeropoulos, and N. Kalogerakis, "Relationship between the carbonyl index (ci) and fragmentation of polyolefin plastics during aging," *Environmental Science and Technology*, vol. 57, pp. 8130–8138, 5 2023. doi: 10.1021/ACS.EST.3C01430.

[75] Anthropic, "claude.ai," Nov. 2024. Available: `https://claude.ai/new`.